# Free-Induction Decays in Solids*†

I. J. Lowe‡ and R. E. Norberg
*Department of Physics, Washington University, St. Louis, Missouri*
(Received March 18, 1957)

A beat structure has been found on free-induction decays associated with the pulsed nuclear magnetic resonance of nuclei in rigid lattices. A general quantum-mechanical theory is developed for the shapes of induction decays. The theory is specialized to the case of rigid solids and applied to the magnetic dipolar interactions among the $F^{19}$ nuclei in a fluorite ($CaF_2$) crystal. It is also shown rigorously that, except at very low temperatures, a free-induction decay is the Fourier transform of the corresponding steady-state resonance line shape. The calculation of the shape of an induction decay in $CaF_2$ thus corresponds to the calculation of the shape of the $F^{19}$ resonance line for the crystal. It is demonstrated that the resonance line shape for an ordered rigid lattice is not Gaussian.

## I. INTRODUCTION

FREE induction or Bloch decays observed in pulsed nuclear magnetic resonance experiments on protons in polyethylene[1,2] and on fluorine nuclei in Teflon exhibit a beat structure when examined at temperatures sufficiently low that large-amplitude nuclear motions have effectively ceased. All solids subsequently examined at liquid nitrogen temperatures (paraffin, ice, zirconium hydride, Lucite, ethyl alcohol, methyl alcohol, and calcium fluoride powders and single crystals) have been found to display a beat modulation of their decay envelopes (Fig. 1).

Induction decay beats previously reported in liquids and solids have arisen either from a chemical shift which produces nuclei with slightly different Larmor frequencies[3] or else from a crystalline lattice structure with several nuclei closer to each other than to other neighbors and thus splitting one another's resonance lines into several components.[4,5] In the case of the solids investigated in the present paper there is no evidence for the existence of any splittings of the c.w. (steady state) line shapes larger than $10^{-5}$ of those required to explain the observed beats. The observed beat frequency is in fact of the order of the full nuclear dipolar coupling.

In the only previous paper which attempts to predict the shape of free-induction decays in solids, Herzog and Hahn[6] assume that the dipole-dipole interactions between nuclei in a solid produce a Gaussian distribution of magnetic fields at the nuclear sites. Their calculation is based on a classical stochastic model and predicts a monotonically decreasing decay without any beat structure.

It was decided that the most suitable approach to the present problem would be to examine a simple solid about which a maximum amount of nuclear resonance information was available. The calcium fluoride crystal ($CaF_2$) was well fitted for this role for the following reasons. All of the abundant isotopes of calcium have zero angular momentum, and therefore have no dipole or quadrupole moments. The only isotope of calcium that has a spin other than zero is $Ca^{43}$, and this is only 0.14% abundant and has a very small magnetic moment. The only stable isotope of fluorine has an angular momentum of $\frac{1}{2}\hbar$, and therefore has no quadrupole moment. The fluorine nuclei form a simple cubic lattice. Furthermore, Pake[7] and Bruce[8] had already made c.w. measurements on the particular cystal used in this experiment and found that its second moment agreed with that predicted by Van Vleck[9] to within a few percent.

Fourier transforms have been calculated of Bruce's[8] c.w. line-shape data for three orientations of the $CaF_2$ crystal with respect to the external field $H_0$. The transforms have been found to have beats and in fact to be identical, within experimental error, to the experimentally observed decay shapes.

In order to interpret the decay measurements made on calcium fluoride, a general theory of free-induction decays has been formulated. The results of the theory are evaluated in this paper for any solid satisfying the conditions that there be only one species of magnetically active nuclei, and that these nuclei have an angular momentum of $\frac{1}{2}\hbar$ and occupy sites rigidly fixed in space.

## II. EXPERIMENTAL PROCEDURE

A standard spin-echo apparatus[10] was employed in the present measurements. A permanent magnet produced a static field of 6890 oersteds in which the Larmor frequency for $F^{19}$ nuclei was 27.6 Mc/sec. The magnet gap was only 1.9 cm which made close control

* This work was supported in part by the Alfred P. Sloan Foundation and by the joint program of the Office of Naval Research and the U. S. Atomic Energy Commission.

† This paper is based on a dissertation submitted by one of us (I.J.L.) to the Department of Physics, Washington University, in partial fulfillment of the requirements for the degree of Doctor of Philosophy.

‡ Alfred P. Sloan Post Doctoral Fellow. During the course of the work reported here, I.J.L. received support as a National Science Foundation Predoctoral Fellow.

1 Lowe, Bowen, and Norberg, Phys. Rev. **100**, 1243 (1955).
2 R. E. Norberg, Bull. Am. Phys. Soc. Ser. II, **1**, 109 (1956).
3 E. L. Hahn and D. E. Maxwell, Phys. Rev. **88**, 1070 (1952).
4 G. E. Pake, J. Chem. Phys. **16**, 327 (1948).
5 T. P. Das and S. K. Ghosh Roy, Indian J. Phys. **29**, 272 (1955).
6 B. Herzog and E. L. Hahn, Phys. Rev. **103**, 148 (1956).
7 G. E. Pake and E. M. Purcell, Phys. Rev. **74**, 1184 (1948).
8 C. R. Bruce, Phys. Rev. **107**, 43 (1957), preceding paper.
9 J. H. Van Vleck, Phys. Rev. **74**, 1168 (1948).
10 E. L. Hahn, Phys. Rev. **80**, 580 (1950).

of the sample temperature quite difficult. The magnet inhomogeneity was about 0.1 oersted over a 1 $cm^2$ sample cross section.

A pulsed rf oscillator-power amplifier transmitter was used and was capable of rotating the $F^{19}$ magnetization through $\pi/2$ in about one microsecond. The sample was placed in one coil arm of a balanced twin-T rf bridge, which served to reduce the amplitude of the rf transmitter pulses arriving at the signal amplifier. The signal amplifier was a commercial 30 Mc/sec I.F. strip manufactured by Linear Equipment Laboratories and designated I.F. 21.

Free-induction decay data were photographed from a Tektronix 531 oscilloscope and measurements made from the photographs. The low temperature measurements were made by immersing the sample and coil directly into a bath of liquid nitrogen contained in a styrofoam vessel.

The calcium fluoride crystal examined was cylindrical in shape and fit the rf coil snugly so as to obtain the largest possible signal-to-noise ratio. The crystal (the same as used in c.w. measurements made by Pake[7] and Bruce[8]) had been cut so that the axis of the cylinder lay along the [110] axis of the crystal. The angle that the [100] axis of the crystal made with the magnetic field was determined by attaching a rod with a pointer to the crystal and then reading the angle from a protractor.

### III. QUANTUM MECHANICS OF FREE-INDUCTION DECAYS

### A. Description of Decays

The quantum-mechanical description of free-induction decays will be given here in as general a form as possible, with restrictions for special cases being introduced as needed.

Let a sample containing $N_0$ identical nuclei be placed in a static magnetic field $H_0\hat{z}$, where $\hat{z}$ is a unit vector in the $z$ direction. The magnetic moment operator and spin operator of the $i$th nucleus will be denoted by $\boldsymbol{\mu}_i$ and $\mathbf{S}_i$, respectively. $\boldsymbol{\mu}_i=\gamma\hbar\mathbf{S}_i$, where $\gamma$ is the gyromagnetic ratio. The total magnetic moment operator of the $N_0$ nuclei is obtained by summation over the $N_0$ nuclei. $\boldsymbol{\mu}=\sum_i\boldsymbol{\mu}_i=\gamma\hbar\sum_i\mathbf{S}_i=\gamma\hbar\mathbf{S}$.

The Hamiltonian for the sample is

$$\mathcal{H}=\mathcal{H}_0+\mathcal{H}_1+\mathcal{H}_2, \tag{1}$$

where $\mathcal{H}_0$ = nuclear Zeeman energy term $=-\gamma\hbar H_0\sum_i S_{iz}=-\gamma\hbar H_0 S_z$, $\mathcal{H}_1$ = total magnetic interaction Hamiltonian among the $N_0$ nuclear magnetic moments, and $\mathcal{H}_2$ = all other parts of the Hamiltonian, such as those due to the motion of the nuclei, the magnetic interaction of the $N_0$ nuclei with electrons and nuclei of other species.

After thermal equilibrium is established, the sample will have developed a macroscopic magnetic moment $\langle\boldsymbol{\mu}\rangle_{Av}$. In Appendix A, formula (A8), it is shown that

$$\langle\boldsymbol{\mu}\rangle_{Av}=\mathrm{Tr}\{\exp(-\mathcal{H}/kT)\boldsymbol{\mu}\}/\mathrm{Tr}\{\exp(-\mathcal{H}/kT)\}, \tag{2}$$

where $T$ is the the temperature of the sample.

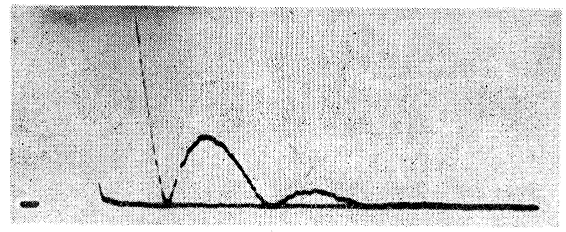

FIG. 1. $F^{19}$ free-induction decay in a $CaF_2$ single crystal. $\mathbf{H}_0$ along [1 0 0]. Temperature 77°K. The visible nulls occur at approximately 22, 43, and 63 $\mu$sec after the rf pulse. The double exposure shows superimposed a second rf pulse which was applied several hundred $\mu$sec after the first pulse in order to check the $\pi/2$ condition of the first pulse. The response to the second pulse also shows a 10-$\mu$sec blocking of the 30-Mc signal amplifier in this case. The beat pattern is distorted by square-law detection.

For the evaluation of Eq. (2), it is assumed that $\mathcal{H}_1\ll\mathcal{H}_0$ and can be ignored. It is further assumed that any spin operator terms in $\mathcal{H}_2$ which refer to the $N_0$ nuclei are small and can also be ignored. That part of $\mathcal{H}_2$ which does not contain any spin operator terms referring to the $N_0$ nuclei will be denoted by $\mathcal{H}_2'$. Since $\mathcal{H}_2'$ commutes with $\mathcal{H}_0$ and since

$$\mathrm{Tr}\{A_{\mathrm{op}}(\mathbf{r}_i)B_{\mathrm{op}}(\mathbf{r}_j)\}=\mathrm{Tr}\{A_{\mathrm{op}}(\mathbf{r}_i)\}\ Tr\{B_{\mathrm{op}}(\mathbf{r}_j)\}$$

where $\mathbf{r}_i$ and $\mathbf{r}_j$ are different sets of variables,

$$\mathrm{Tr}\{\exp(-\mathcal{H}_2'/kT)\}$$

cancels out of the calculation. If one substitutes into the resulting equation the definitions of $\mathcal{H}_0$ and $\boldsymbol{\mu}$, one finds

$$\langle\boldsymbol{\mu}\rangle_{Av}=\frac{\mathrm{Tr}\{\exp(\zeta\sum_i S_{iz})\gamma\hbar\sum_j(S_{jz}\hat{z})\}}{\mathrm{Tr}\{\exp(\zeta\sum_i S_{iz})\}}+\frac{\mathrm{Tr}\{\exp(\zeta\sum_i S_{iz})\gamma\hbar\sum_j(S_{jx}\hat{x}+S_{jy}\hat{y})\}}{\mathrm{Tr}\{\exp(\zeta\sum_i S_{iz})\}}, \tag{3}$$

where $\zeta=(\gamma\hbar H_0/kT)$.

The trace of a matrix is independent of basis. If one chooses the basis in which each spin is individually quantized along the $z$ axis, the trace associated with the $x$ and $y$ components vanishes, and

$$\langle\boldsymbol{\mu}\rangle_{Av}=\frac{\gamma\hbar\hat{z}\sum_j\mathrm{Tr}\{(\prod_i e^{\zeta S_{iz}})S_{jz}\}}{\mathrm{Tr}\{\prod_i e^{\zeta S_{iz}}\}}, \tag{4}$$

which may be rewritten as

$$\langle\boldsymbol{\mu}\rangle_{Av}=\gamma\hbar H_0\hat{z}\sum_j\frac{\mathrm{Tr}\{e^{\zeta S_{jz}}S_{jz}\}}{\mathrm{Tr}\{e^{\zeta S_{jz}}\}}=-N_0\gamma\hbar\hat{z}T\zeta^{-1}\frac{\partial}{\partial T}[\ln(\sum_{s'=-s}^{s}e^{\zeta s'})]. \tag{5}$$

TABLE I. The transformation properties of the spin operators to rotations about the $x$, $y$, and $z$ axes.

| | Rotation about $x$ axis | Rotation about $y$ axis | Rotation about $z$ axis |
|---|---|---|---|
| $R(\theta)$ | $e^{i\theta S_x}$ | $e^{i\theta S_y}$ | $e^{i\theta S_z}$ |
| $s_x'$ | $S_x$ | $S_x\cos\theta - S_z\sin\theta$ | $S_x\cos\theta + S_y\sin\theta$ |
| $s_y'$ | $S_y\cos\theta + S_z\sin\theta$ | $S_y$ | $S_y\cos\theta - S_x\sin\theta$ |
| $s_z'$ | $S_z\cos\theta - S_y\sin\theta$ | $S_z\cos\theta + S_x\sin\theta$ | $S_z$ |

The terms on the right-hand side of Eq. (5) form a geometric progression containing $2s+1$ terms, having a ratio factor of $\exp(-\zeta)$ and a first term of $\exp(\zeta S)$. Therefore

$$\langle\boldsymbol{\mu}\rangle_{\mathrm{Av}} = N_0\gamma\hbar\hat{z}\{\tfrac{1}{2}(2s+1)\coth[\tfrac{1}{2}(2s+1)\zeta] - \tfrac{1}{2}\coth(\tfrac{1}{2}\zeta)\}. \quad (6)$$

Equation (6) agrees with the Langevin value and its magnitude will henceforth be denoted by $\mu(0)$. Its high-temperature approximation, $N_0(\gamma\hbar)^2 s(s+1)H_0/3kT$, will be denoted by $\mu'(0)$. (The high-temperature approximation is valid for $(2s+1)\zeta/2 \ll 1$.)

After the sample is placed in a magnetic field and allowed to reach thermal equilibrium, a "$\pi/2$" rf magnetic field pulse $H_1(t')$ is applied in the $x,y$ plane. The pulse nutates the macroscopic magnetic moment into the $x,y$ plane. The rf pulse will be assumed to have a square envelope, at last $t_w$ seconds, and to have a carrier frequency $f_0$ equal to the Larmor frequency. For the sake of convenience, the phase of the rf pulse will be chosen such that

$$\mathbf{H}_1(t') = H_1[(\sin\omega_0 t')\hat{x} + (\cos\omega_0 t')\hat{y}]$$

where $t'$ is the time measured from the beginning of the rf pulse. The Hamiltonian describing the sample while the rf pulse is on is $\mathcal{H}'(t') = \mathcal{H} + \mathcal{H}_3(t')$, where

$$\mathcal{H}_3(t') = -\boldsymbol{\mu}\cdot\mathbf{H}_1(t') = -\hbar\omega_1(S_x\sin\omega_0 t' + S_y\cos\omega_0 t'),$$

with $\omega_1 = \gamma H_1$.

The wave function describing the sample while the rf pulse is on will be denoted by $\psi(t')$. It satisfies the Schrödinger equation, $\mathcal{H}'(t')\psi(t') = i\hbar\partial\psi'(t')/\partial t'$. Since the wave function describing the sample cannot change instantaneously, $\psi(t')]_{t'=0}$ must satisfy the initial condition that it be identical to the wave function $\kappa$ describing the sample immediately before the rf pulse is turned on.

Let $\psi(t') = \exp(it'\mathcal{H}/\hbar)\psi'(t')$, so that

$$\exp(it'\mathcal{H}/\hbar)\mathcal{H}_3(t')\exp(-it'\mathcal{H}/\hbar)\psi'(t') = i\hbar\partial\psi'(t')/\partial t'. \quad (7)$$

It is now assumed that $t_w$ is sufficiently small that those terms in $\mathcal{H}_1$ and $\mathcal{H}_2$ which do not commute with $\mathcal{H}_3(t')$ or $\mathcal{H}_0$ have expectation values which are much less than 1 when multiplied by $t_w/\hbar$. Their effect upon $\mathcal{H}_3(t')$ may then be ignored. This procedure is equivalent to the assumption that the Fourier spectrum of the rf pulse is much broader than the Larmor frequency deviations of the individual nuclei. The Larmor frequency deviations in question arise from the "local field inhomogeneities induced" by $\mathcal{H}_1$ and $\mathcal{H}_2$. Thus there are left only those $\mathcal{H}_1$ and $\mathcal{H}_2$ terms in

$$\exp[-it(\mathcal{H}_0 + \mathcal{H}_1 + \mathcal{H}_2)/\hbar]$$

that do commute with $\mathcal{H}_3(t')$ and $\mathcal{H}_0$, and Eq. (7) may be reduced to

$$-e^{-i\omega_0 t' S_z}[\omega_1(S_x\sin\omega_0 t' + S_y\cos\omega_0 t')] \times e^{i\omega_0 t' S_z}\psi'(t') = i\partial\psi'(t')/\partial t'. \quad (8)$$

The quantity $\exp(i\omega_0 t' S_z)$ is just the operator $R_z(\omega_0 t')$ for rotation about the $z$ axis. It is easy to demonstrate that the transformation properties of the spin operators are those given in Table I.

Using Table I, Eq. (8) reduces to

$$i\omega_1 S_y\psi'(t') = \partial\psi'(t')/\partial t',$$

the solution of which is $\psi'(t') = \exp(i\omega_1 S_y t')\psi'(0)$. To satisfy the previously mentioned initial condition, $\psi(0)$ is chosen to be identical to the wave function $\kappa(0)$ describing the system immediately before the rf pulse is turned on. Then

$$\psi(t_w) = \exp(-it_w\mathcal{H}_2'/\hbar)e^{i\omega_0 t_w S_z}e^{i\omega_1 t_w S_y}\kappa(0).$$

The wave function describing the sample after the rf pulse is turned off will be denoted by $\phi(t)$, where the origin of $t$ is the instant at which the pulse is turned off. Since the wave function describing the sample cannot change instantaneously, $\phi(t)$ must satisfy the initial condition that it be identical to the wave function describing the sample immediately before the rf pulse is turned off; that is, $\phi(0) = \psi(t_w)$.

Therefore, for $t_w$ short enough, the action of the rf pulse upon the sample is well approximated by a simple operator. $\mathrm{Exp}(i\omega_0 t_w S_z)$ represents the precession of the spins about $H_0\hat{z}$ and $\exp(i\omega_1 t_w S_y)$ represents the precession of the spins about $\mathbf{H}_1$. The nutation produced by the rf pulse is made to satisfy the "$\pi/2$" condition by setting $\gamma H_1 t_w = \pi/2$.

In Appendix A, it is shown that $t$ seconds after the "$\pi/2$" pulse is turned off

$$\langle\boldsymbol{\mu}(t)\rangle_{\mathrm{Av}} = \frac{\mathrm{Tr}\{\exp(-\mathcal{H}/kT)\exp(it_w\mathcal{H}_2'/\hbar)R_{\mathrm{op}}^{\dagger}(t_w)T_{\mathrm{op}}^{\dagger}(t)\boldsymbol{\mu}T_{\mathrm{op}}(t)R_{\mathrm{op}}(t_w)\exp(-it_w\mathcal{H}_2'/\hbar)\}}{\mathrm{Tr}\{\exp(-\mathcal{H}/kT)\}}, \quad (9)$$

where $T_{\mathrm{op}}(t) = \exp(-it\mathcal{H}/\hbar)$ and $R_{\mathrm{op}}(t_w) = \exp(i\omega_0 t_w S_z)\exp(iS_y\pi/2)$.

Since $\mathrm{Tr}(A_{\mathrm{op}}B_{\mathrm{op}}) = \mathrm{Tr}(B_{\mathrm{op}}A_{\mathrm{op}})$, where $A_{\mathrm{op}}$ and $B_{\mathrm{op}}$ are any two operators, Eq. (9) may be rewritten in the form

$$\langle\boldsymbol{\mu}(t)\rangle_{\mathrm{Av}} = \frac{\mathrm{Tr}\{\exp(-it_w\mathcal{H}_2'/\hbar)\exp(-\mathcal{H}/kT)\exp(it_w\mathcal{H}_2'/\hbar)R_{\mathrm{op}}^{\dagger}(t_w)T_{\mathrm{op}}^{\dagger}(t)\boldsymbol{\mu}T_{\mathrm{op}}(t)R_{\mathrm{op}}(t_w)\}}{\mathrm{Tr}\{\exp(-\mathcal{H}/kT)\}}. \quad (10)$$

Equation (10) can easily be evaluated for $t=0$ by using the technique previously applied to Eq. (2). Equation (10) then reduces to

$$\langle\boldsymbol{\mu}(0)\rangle_{\mathrm{Av}}=N_0\gamma\hbar\{\tfrac{1}{2}(2s+1)\coth[\tfrac{1}{2}(2s+1)\zeta] -\tfrac{1}{2}\coth\tfrac{1}{2}\zeta\}\{-(\cos\omega_0 t_w)\hat{x}+(\sin\omega_0 t_w)\hat{y}\}. \quad (11)$$

Therefore the macroscopic magnetization has nutated from along the $z$ axis into the $x,y$ plane. While doing so, it has also performed $t_w/f_0$ revolutions about the $z$ axis, and at the end of the pulse, makes an angle $\omega_0 t_w$ with respect to $-\hat{x}$. Since the system has cylindrical symmetry about the applied static magnetic field, the initial azimuthal angle which the macroscopic magnetization makes with the $-x$ axis should not affect the rate of decay of the macroscopic magnetization. To simplify later calculations, this angle will be assumed to be $(2p+1)\pi$, where $p$ is an integer. Then $\langle\boldsymbol{\mu}(0)\rangle_{\mathrm{Av}}=\mu(0)\hat{x}$.

In the usual free-induction decay experiment, a single receiver coil is oriented perpendicular to the static magnetic field. With no loss of generality, one may assume the $x$ axis of the laboratory coordinate system to be along the coil axis. This coil is responsive only to changing magnetic fields along the $x$ axis and one need only evaluate $\langle\mu_x(t)\rangle_{\mathrm{Av}}$ since this is the physical quantity observed. Therefore, the general quantum-mechanical formula predicting the shape of the decay for a particular species of nuclei in any substance at any temperature is given by the $x$ component of Eq. (10).

Another useful result derivable from Eq. (10) is the rate of relaxation of the spins, after the "$\pi/2$" pulse, toward the direction of the static magnetic field. The time constant $T_1$ associated with this process describes the rate of growth of the $z$ component of the macroscopic magnetization $\langle\mu_z(t)\rangle_{\mathrm{Av}}$ and is derivable from the $z$ component of Eq. (10).

### B. High-Temperature Relationship between the Free-Induction Decay and the Spectral Density Function

Let the shape function of a spectral line be $g(\omega)$, where

$$\int_{-\infty}^{\infty} g(\omega)d\omega=1.$$

Let $F(t)$ be the Fourier transform of the shape function $g(\omega)$. Then

$$F(t)=\int_{-\infty}^{\infty} e^{-i\omega t}g(\omega)d\omega=\int_{-\infty}^{\infty}\sum_{n=0}^{\infty}\frac{(-i\omega t)^n}{n!}g(\omega)d\omega =\sum_{n=0}^{\infty}\frac{(-it)^n}{n!}\langle\omega^n\rangle. \quad (12)$$

One is concerned with the magnetic dipole radiation linearly polarized parallel to the $x$ axis. The probability of the radiation producing a net absorption between levels $a$ and $b$ (assumed to have negligible widths) is proportional to $|\langle\psi_a|\mu_x|\psi_b\rangle|^2\exp(-E_a/kT)$.[11]

The mean $n$th absorption frequency is the sum of absorption frequencies raised to the $n$th power and summed, each frequency being weighted by its transition probability,

$$\langle\omega^n\rangle=\frac{\sum_{a,b}\omega_{a,b}{}^n|\langle\psi_b|\mu_x|\psi_a\rangle|^2e^{-E_a/kT}}{\sum_{a,b}|\langle\psi_b|\mu_x|\psi_a\rangle|^2e^{-E_a/kT}}, \quad (13)$$

where $\omega_{a,b}=(E_a-E_b)/\hbar$.

Equation (13), without the Boltzmann factors, is just the starting point of the Van Vleck method of moments.[9]

Substituting Eq. (13) into (12), one obtains

$$F(t)=\frac{\sum_{a,b}\langle\psi_a|e^{-E_a/kT}\mu_x|\psi_b\rangle\langle\psi_b|e^{itE_b/\hbar}\mu_x e^{-itE_a/\hbar}|\psi_a\rangle}{\sum_{a,b}\langle\psi_a|e^{-E_a/kT}\mu_x|\psi_b\rangle\langle\psi_b|\mu_x|\psi_a\rangle} =\frac{\mathrm{Tr}\{\exp(-\mathcal{H}/kT)\mu_x(0)\mu_x(t)\}}{\mathrm{Tr}\{\exp(-\mathcal{H}/kT)\mu_x{}^2(0)\}}. \quad (14)$$

Thus one sees that the Fourier transform of the shape function of the absorption line, excluding the Boltzmann factor, is nothing other than the autocorrelation function of the associated dipole moment. This result, without however inclusion of the $\exp(-\mathcal{H}/kT)$ factor, has also been derived by Yokota[12] as a suggested technique of calculation for pressure broadening of microwave spectra.

Suppose now that the temperature of the sample is high enough that one may ignore $\mathcal{H}_0+\mathcal{H}_1+(\mathcal{H}_2-\mathcal{H}_2')$ while evaluating $\exp(-\mathcal{H}/kT)$ in Eq. (14). (This is equivalent to assuming that the sets of energy levels generated by these terms are all equally populated.) Then

$$F(t)=\frac{\mathrm{Tr}\{\exp(-\mathcal{H}_2'/kT)S_x(0)S_x(t)\}}{\tfrac{1}{3}N_0 s(s+1)(2s+1)^{N_0}\,\mathrm{Tr}\{\exp(-\mathcal{H}_2'/kT)\}}, \quad (15)$$

where the leading terms in the denominator correspond to $\mathrm{Tr}[S_x{}^2(0)]$.

It will now be demonstrated that the general expression for the free induction decay, the $\langle\mu_x(t)\rangle_{\mathrm{Av}}$ from Eq. (10), is equal to $\mu'(0)F(t)$ in the approximation that $\mathcal{H}_1\ll\mathcal{H}_0$ and $\mathcal{H}_2\approx\mathcal{H}_2'$. In this approximation, Eq. (10) may be written

[11] M. H. L. Pryce and K. W. H. Stevens, Proc. Phys. Soc. (London) **A63**, 36 (1950).

[12] I. Yokota, Progr. Theoret. Phys. Japan **8**, 380 (1952).

$$\langle\mu_x(t)\rangle_{\text{Av}}=\frac{\text{Tr}\{\exp(-\mathcal{H}_2'/kT)\exp(-\mathcal{H}_0/kT)R_{\text{op}}^{\dagger}(t_w)\mu_x(t)R_{\text{op}}(t_w)\}}{\text{Tr}\{\exp(-\mathcal{H}_0/kT)\exp(-\mathcal{H}_2'/kT)\}}=\frac{\text{Tr}\{\exp(-\mathcal{H}_2'/kT)e^{i\pi S}e^{i\frac{1}{2}\pi S_y}e^{\zeta S_z}e^{-i\frac{1}{2}\pi S_y}e^{-i\pi S_z}\mu_x(t)\}}{\text{Tr}\{\exp(-\mathcal{H}_0/kT)\exp(-\mathcal{H}_2'/kT)\}}. \tag{16}$$

Using Table I, one finds that

$$\langle\mu_x(t)\rangle_{\text{Av}}=\frac{\gamma\hbar\,\text{Tr}\{\exp(-\mathcal{H}_2'/kT)e^{\zeta S_x}S_x(t)\}}{\text{Tr}\{\exp(-\mathcal{H}_2'/kT)\}\,\text{Tr}\{\exp(-\mathcal{H}_0/kT)\}}. \tag{17}$$

As in the case of the spectral density function, it is assumed that $\zeta\ll 1$. Therefore

$$e^{\zeta S_x}\cong\prod_{i=1}^{N_0}(1+\zeta S_{ix}) \tag{18}$$

and

$$\langle\mu_x(t)\rangle_{\text{Av}}=\frac{\gamma\hbar\,\text{Tr}\{\exp(-\mathcal{H}_2'/kT)\prod_i(1+\zeta S_{ix})S_x(t)\}}{\text{Tr}\{\exp(-\mathcal{H}_2'/kT)\}\prod_i\text{Tr}\{1+\zeta S_{iz}\}}. \tag{19}$$

However, $\text{Tr}(1_{\text{op}})=(2s+1)$ (for the $i$th set of wave functions), $\text{Tr}(S_{ix})=0$, $\text{Tr}[\exp(-\mathcal{H}_2'/kT)S_x(t)]=0$, and $\text{Tr}[\exp(-\mathcal{H}_2'/kT)S_{kz}(0)S_{lx}(0)S_{jx}(0)\cdots]=0$ for $(k\neq l\neq m\neq\cdots)$. Therefore one finds that

$$\langle\mu_x(0)\rangle_{\text{Av}}=\gamma\hbar\zeta\frac{\text{Tr}\{\exp(-\mathcal{H}_2'/kT)\sum_{j,k}S_{jx}(0)S_{kx}(0)\}}{(2s+1)^{N_0}\,\text{Tr}\{\exp(-\mathcal{H}_2'/kT)\}}. \tag{20}$$

with the terms of higher order than the first making no contributions. For $t>0$, $S_{jx}(t)$ is a function of the spin operators $S_{kx}(0)$, $S_{lx}(0)$, $\cdots$. Therefore there is some correlation of $S_{jx}(t)$ with $S_{kx}(0)$, $S_{lx}(0)$, $\cdots$, etc., and $\text{Tr}[\exp(-\mathcal{H}_2'/kT)\,S_{kx}(0)S_{lx}(0)S_{jx}(t)\cdots]$ does not necessarily vanish. If the interaction between spins is of a short-range nature, then the contributions of the higher-order terms are still small. To show this, assume that $S_{jx}(t)$ is influenced by only $N'$ near neighbors, and that the influence of each of these neighbors may be approximated by a correlation function $c(t)$. Then

$$\zeta^2\sum_{\substack{j,k,l\\k\neq l}}\text{Tr}\{\exp(-\mathcal{H}_2'/kT)S_{kx}(0)S_{lx}(0)S_{jx}(t)\}\simeq 2\zeta^2C(t)N'\sum_{j,k}\text{Tr}\{\exp(-\mathcal{H}_2'/kT)S_{kx}(0)S_{jx}(t)\}. \tag{21}$$

If $2\zeta c(t)N'\ll 1$ for all $t$, then expression (21) is negligible in comparison to

$$\zeta\sum_{j,k}\text{Tr}[\exp(-\mathcal{H}_2'/kT)S_{kx}(0)S_{jx}(t)]$$

and may be ignored. The same argument holds true for the higher order terms except that the product containing $n$ $S_{kx}(0)$ terms will end up with a coefficient smaller than $[\zeta c(t)N']^{n-1}$. Thus, only the first term of this series makes a major contribution to $\langle\mu_x(t)\rangle_{\text{Av}}$ and

$$\langle\mu_x(t)\rangle_{\text{Av}}=\frac{\gamma\hbar\zeta\,\text{Tr}\{\exp(-\mathcal{H}_2'/kT)S_x(0)S_x(t)\}}{(2s+1)^{N_0}\,\text{Tr}\{\exp(-\mathcal{H}_2'/kT)\}}. \tag{22}$$

Comparing Eqs. (22) and (15), one finds that

$$\langle\mu_x(t)\rangle_{\text{Av}}=\mu'(0)F(t). \tag{23}$$

Thus, as was to be proven, the Fourier transform of the spectral density function is identical to the expression for the free-induction decay to within a multiplying constant at a high enough temperature ($\zeta\ll 1$; i.e., $T>0.1°\text{K}$ for $H_0\simeq 10^4$ gauss). This theorem holds for solids, liquids, and gases, and for any type of short-range interaction between the particles making up the sample.

Equation (12) may be restated as $F(t)=\langle\exp(-i\omega t)\rangle$ and Eq. (23) can then be rewritten as

$$\langle\mu_x(t)\rangle_{\text{Av}}=\mu'(0)\langle e^{-i\omega t}\rangle. \tag{24}$$

One may therefore consider a free-induction decay to be just the expectation value of the phase function of the Larmor frequency of all the $N_0$ nuclei of the sample. From Eq. (22), one finds that

$$\langle\mu_x(-t)\rangle_{\text{Av}}=\frac{\gamma\hbar\zeta\,\text{Tr}\{\exp(-\mathcal{H}_2'/kT)S_x(0)\exp(-it\mathcal{H}/\hbar)S_x(0)\exp(it\mathcal{H}/\hbar)\}}{(2s+1)^{N_0}\,\text{Tr}\{\exp(-\mathcal{H}_2'/kT)\}}. \tag{25}$$

It will be assumed for the evaluation of Eq. (25) that

$$\exp(it\mathcal{H}/\hbar)\exp(-\mathcal{H}_2'/kT)\simeq\exp(-\mathcal{H}_2'/kT)\exp(it\mathcal{H}/\hbar).$$

Therefore, $\langle\mu_x(t)\rangle_{\text{Av}}$ is an even-valued function of $t$, and

$$\langle\mu_x(t)\rangle_{\text{Av}}=\mu'(0)\langle\cos(\omega_0+\Delta\omega)t\rangle\quad(\text{where }\omega-\omega_0=\Delta\omega)$$
$$=\mu'(0)\left\{\cos\omega_0t\sum_{\text{even }n}\frac{(it)^n}{n!}\langle(\Delta\omega)^n\rangle-\sin\omega_0t\sum_{\text{odd n}}\frac{(it)^n}{in!}\langle(\Delta\omega)^n\rangle\right\}. \tag{26}$$

Equation (26) will be useful for comparing the results of Sec. IV with those of Van Vleck.[9] If the high-temperature condition is not satisfied, then the various expansions involving $\zeta$ are not permissible and $\langle\mu_x(t)\rangle_{\text{Av}}\neq\mu'(0)F(t)$.

## IV. FREE-INDUCTION DECAY CALCULATIONS FOR A RIGID CRYSTALLINE SOLID

### A. Hamiltonian

For the calculation carried out in this section, it will be assumed that the sample contains only one species of particle having a magnetic moment, and that these are nuclei. The nuclear magnetic interaction among these nuclei may be expressed in the following way.[9]

$$\mathcal{H}_1=-\sum_{k<j} 2J_{jk}\mathbf{S}_j\cdot\mathbf{S}_k+(\gamma\hbar)^2\sum_{k<j}\left[-\frac{8\pi}{3}\mathbf{S}_j\cdot\mathbf{S}_k\delta(r_{jk})+\frac{\mathbf{S}_j\cdot\mathbf{S}_k}{r_{jk}^3}-\frac{3(\mathbf{S}_j\cdot\hat{r}_{jk})(\mathbf{S}_k\cdot\hat{r}_{jk})}{r_{jk}^3}\right]. \quad (27)$$

Here $\mathbf{r}_{jk}$ is the vector connecting the positions of the $j$th and $k$th nuclei, and $J_{jk}$ is the usual exchange integral. The first term in the above expression is the exchange interaction term arising from the possibility of two identical particles "exchanging places." The second term is the dipole-dipole interaction term, including the Fermi hyperfine term.

At sufficiently low temperatures, all the nuclear motion in a solid is vibrational and of small amplitude. Such nuclear motion does not effectively average out dipole-dipole interactions, nor destroy the coherence of spin processes. It is therefore permissible to assume that $\mathcal{H}_2$ and $\mathcal{H}_1$ commute for the evaluation of free-induction decays of solids at these temperatures. Since $\mathcal{H}_2$ commutes with $\mathcal{H}_0$ and $\mu_x$, one has

$$\exp(-it_w\mathcal{H}_2'/\hbar)\exp(-\mathcal{H}/kT)\exp(it_w\mathcal{H}_2'/\hbar)=\exp(-\mathcal{H}/kT)$$

and formula (10) may be reduced to

$$\langle\mu_x(t)\rangle_{\text{Av}}=\frac{\text{Tr}\{\exp[-(\mathcal{H}_0+\mathcal{H}_1)/kT]R_{\text{op}}^\dagger(t_w)\exp[it(\mathcal{H}_0+\mathcal{H}_1)/\hbar]\mu_x\exp[-it(\mathcal{H}_0+\mathcal{H}_1)/\hbar]R_{\text{op}}(t_w)\}}{\text{Tr}\{\exp[-(\mathcal{H}_0+\mathcal{H}_1)/kT]\}}. \quad (28)$$

The direction cosines of $\mathbf{r}_{jk}$ relative to the laboratory frame of reference are now defined as $(\alpha_{jk},\beta_{jk},\gamma_{jk})$. If $S_+=S_x+iS_y$ and $S_-=S_x-iS_y$, then

$$\mathbf{S}_j\cdot\mathbf{S}_k=\tfrac{1}{2}(S_{j+}S_{k-}+S_{j-}S_{k+})+S_{jz}S_{kz}.$$

$\mathcal{H}_1$ may then be rewritten as[13]

$$\mathcal{H}_1=\sum_{k<j}[A_{jk}\mathbf{S}_j\cdot\mathbf{S}_k+B_{jk}S_{jz}S_{kz}+C_{jk}(S_{j+}S_{kz}+S_{jz}S_{k+})+D_{jk}(S_{j-}S_{kz}+S_{jz}S_{k-})+E_{jk}S_{j+}S_{k+}+F_{jk}S_{j-}S_{k-}], \quad (29)$$

where

$$A_{jk}=-2J_{jk}-\frac{8\pi}{3}(\gamma\hbar)^2\delta(r_{jk})-\frac{(\gamma\hbar)^2}{2r_{jk}^3}(1-3\gamma_{jk}^2)=A_{kj},$$

$$B_{jk}=3[(\gamma\hbar)^2/2r_{jk}^3](1-3\gamma_{jk}^2)=B_{kj},$$

$$C_{jk}=-\tfrac{3}{2}[(\gamma\hbar)^2/r_{jk}^3]\gamma_{jk}(\alpha_{jk}-i\beta_{jk}),$$

$$D_{jk}=-\tfrac{3}{2}[(\gamma\hbar)^2/r_{jk}^3]\gamma_{jk}(\alpha_{jk}+i\beta_{jk}),$$

$$E_{jk}=-\tfrac{3}{4}[(\gamma\hbar)^2/r_{jk}^3](\alpha_{jk}^2-2i\alpha_{jk}\beta_{jk}-\beta_{jk}^2),$$

$$F_{jk}=-\tfrac{3}{4}[(\gamma\hbar)^2/r_{jk}^3](\alpha_{jk}^2+2i\alpha_{jk}\beta_{jk}-\beta_{jk}^2).$$

If $\mathcal{H}_1'$ denotes $\mathcal{H}_1$ transformed to the Larmor rotating reference frame whose $z$ axis coincides with the $z$ axis of the laboratory reference frame, and whose $x$ and $y$ axes are rotating about the $z$ axis with an angular velocity $\omega_0\hat{z}$, it can be shown from Table I that

$$\mathcal{H}_1'=\sum_{k<j}[A_{jk}\mathbf{S}_j\cdot\mathbf{S}_k+B_{jk}S_{jz}S_{kz}+C_{jk}(S_{j+}S_{kz}+S_{jz}S_{k+})e^{-i\omega_0t}+D_{jk}(S_{j-}S_{kz}+S_{jz}S_{k-})e^{i\omega_0t}+E_{jk}S_{j+}S_{k+}e^{-2i\omega_0t}+F_{jk}S_{j-}S_{k-}e^{2i\omega_0t}]. \quad (30)$$

It is found experimentally that the nuclei of a particular species have a distribution of Larmor frequencies with a half-width of no more than 1% in a sample free of paramagnetic impurities in a static magnetic field of 1000 oersteds or more. In the previously discussed solid where the nuclei may be considered to be fixed in space, these spins when viewed from the Larmor rotating reference frame will have little relative motion with respect to one another or the observer. The most effective terms of $\mathcal{H}_1'$ are therefore those that are time-independent in the rotating frame since the time-dependent terms will be effectively averaged out over a short interval of time (such as several Larmor periods). Consequently the time-dependent terms of $\mathcal{H}_1'$ will be dropped from future calculations of this section. Van Vleck,[9] in his evaluation of the second and fourth moments for a solid, also dropped these same terms because of their nonsecular behavior. Thus, there remain only those components of $\mathcal{H}_1$ which are secular in the rotating reference frame:

$$\mathcal{H}_1''=\tfrac{1}{2}\sum_{j\neq k}(A_{jk}\mathbf{S}_j\cdot\mathbf{S}_k+B_{jk}S_{jz}S_{kz}). \quad (31)$$

It is further assumed for the evaluation of

$$\exp[-(\mathcal{H}_0+\mathcal{H}_1)/kT]$$

in Eq. (28) that $\mathcal{H}_1$ is much less than $\mathcal{H}_0$ and may be ignored. It is easily shown that $\mathcal{H}_0$ and $\mathcal{H}_1''$ commute. Therefore

$$\langle\mu_x(t)\rangle_{\text{Av}}=\frac{\gamma\hbar\,\text{Tr}\{\exp(-\mathcal{H}_0/kT)R_{\text{op}}^\dagger(t_w)\exp(it\mathcal{H}_1''/\hbar)\exp(it\mathcal{H}_0/\hbar)S_x\exp(-it\mathcal{H}_0/\hbar)\exp(-it\mathcal{H}_1''/\hbar)R_{\text{op}}(t_w)\}}{\text{Tr}\{\exp(-\mathcal{H}_0/kT\}}. \quad (32)$$

[13] In a slight modification of a notation used by Van Vleck (reference 9).

It was shown in the previous section that

$$R_{\rm op}(t_w)=\exp(i\pi S_z)\exp(\tfrac{1}{2}i\pi S_y).$$

Using the results of Table I, we obtain

$$\exp(it\mathcal{H}_0/\hbar)S_x\exp(-it\mathcal{H}_0/\hbar)=S_x\cos\omega_0t+S_y\sin\omega_0t,\quad(33)$$

$$R_{\rm op}^\dagger(t_w)\exp(it\mathcal{H}_0/\hbar)S_x\exp(-it\mathcal{H}_0/\hbar)R_{\rm op}(t_w)=S_z\cos\omega_0t-S_y\sin\omega_0t,\quad(34)$$

and

$$R_{\rm op}^\dagger(t_w)\exp(it\mathcal{H}_1'')R_{\rm op}(t_w)=\exp[-(it/2\hbar)\sum_{j\neq k}(A_{jk}\mathbf{S}_j\cdot\mathbf{S}_k+B_{jk}S_{jx}S_{kx})].\quad(35)$$

Therefore

$$\langle\mu_x(t)\rangle_{\rm Av}=\gamma\hbar\cos\omega_0t\frac{\mathrm{Tr}\{\exp(-\mathcal{H}_0/kT)e^{it(\alpha+\beta)}S_ze^{-it(\alpha+\beta)}\}}{\mathrm{Tr}\{\exp(-\mathcal{H}_0/kT)\}}-\gamma\hbar\sin\omega_0t\frac{\mathrm{Tr}\{\exp(-\mathcal{H}_0/kT)e^{it(\alpha+\beta)}S_ye^{-it(\alpha+\beta)}\}}{\mathrm{Tr}\{\exp(-\mathcal{H}_0/kT)\}},\quad(36)$$

where

$$\alpha=\frac{1}{2\hbar}\sum_{j\neq k}A_{jk}\mathbf{S}_j\cdot\mathbf{S}_k,$$

$$\beta=\frac{1}{2\hbar}\sum_{j\neq k}B_{jk}S_{jx}S_{kx}.$$

If $\alpha=\beta=0$ (no magnetic interaction between nuclei), then

$$\langle\mu_x(t)\rangle_{\rm Av}=\gamma\hbar\left(\cos\omega_0t\frac{\mathrm{Tr}\{\exp(-\mathcal{H}_0/kT)S_z\}}{\mathrm{Tr}\{\exp(-\mathcal{H}_0/kT)\}}-\sin\omega_0t\frac{\mathrm{Tr}\{\exp(-\mathcal{H}_0/kT)S_y\}}{\mathrm{Tr}\{\exp(-\mathcal{H}_0/kT)\}}\right).\quad(37)$$

As in Eq. (2), Eq. (37) may be immediately evaluated as $\langle\mu_x(t)\rangle_{\rm Av}=\mu(0)\cos\omega_0t$. Therefore, in the case of vanishing magnetic interaction between nuclei, the macroscopic magnetization of the sample, subsequent to its nutation into the $x,y$ plane, precesses about the $z$ axis with the angular speed $\gamma H_0$ without diminishing in magnitude. This same result is derivable in a much simpler manner by using the vector model.[10]

### B. Decay Shapes for Special Values of $A_{jk}$ and $B_{jk}$

The evaluation of Eq. (36) is hampered by the fact that $\alpha$ and $\beta$ do not commute. ($[\alpha,\beta]_-$ is evaluated in Appendix B.) Since the coefficients of operators in $\alpha$ and $\beta$ are of the same order of magnitude, one cannot use any expansion technique for $\exp[-it(\alpha+\beta)]$ based upon one of the two quantities being much smaller than the other. A different criterion for expansion will be developed in this section from an examination of the two special cases: all $B_{jk}$ independent of $j$ and $k$, and $A_{jk}=0$ for all $j$ and $k$.

The results of Appendix B show that, for the spin $\frac{1}{2}$ case, $[\alpha,\beta]_-=0$ if $B_{jk}$ is independent of $j$ and $k$. In this case $\exp[-it(\alpha+\beta)]=\exp(-it\alpha)\exp(-it\beta)$ and

$$\langle\mu_x(t)\rangle_{\rm Av}=\gamma\hbar\cos\omega_0t\frac{\mathrm{Tr}\{\exp(-\mathcal{H}_0/kT)e^{it\beta}e^{it\alpha}S_ze^{-it\alpha}e^{-it\beta}\}}{\mathrm{Tr}\{\exp(-\mathcal{H}_0/kT)\}}-\gamma\hbar\sin\omega_0t\frac{\mathrm{Tr}\{\exp(-\mathcal{H}_0/kT)e^{it\beta}e^{it\alpha}S_ye^{-it\alpha}e^{-it\beta}\}}{\mathrm{Tr}\{\exp(-\mathcal{H}_0/kT)\}}.\quad(38)$$

It is easy to show that $[\alpha,S_x]_-=[\alpha,S_y]_-=[\alpha,S_z]_-=0$ (this follows at once from the rotational invariance of $\alpha$). The above expression then reduces to

$$\langle\mu_x(t)\rangle_{\rm Av}=\gamma\hbar\left[\cos\omega_0t\frac{\mathrm{Tr}\{\exp(-\mathcal{H}_0/kT)e^{it\beta}S_ze^{-it\beta}\}}{\mathrm{Tr}\{\exp(-\mathcal{H}_0/kT)\}}-\sin\omega_0t\frac{\mathrm{Tr}\{\exp(-\mathcal{H}_0/kT)e^{it\beta}S_ye^{-it\beta}\}}{\mathrm{Tr}\{\exp(-\mathcal{H}_0/kT)\}}\right].\quad(39)$$

Thus for $s=\frac{1}{2}$ and $B_{jk}$ independent of $j$ and $k$, the shape of the decay is independent of the $A_{jk}$'s. This fact was first pointed out by Van Vleck[9] in a different way. He demonstrated that the moments of a spectral density function are independent of $A_{jk}$ if $B_{jk}$ is independent of $j$ and $k$. For $s$ greater than $\frac{1}{2}$, $[\alpha,\beta]_-$ is zero only for $\alpha$ or $\beta=0$. If $\beta=0$, $\langle\mu_x(t)\rangle_{\rm Av}$ can be shown to be independent of $\alpha$ by the same argument as was used above.

In the special case that $A_{jk}=0$ for all $j$ and $k$,

$$\langle\mu_x(t)\rangle_{\rm Av}=\gamma\hbar\cos\omega_0t\frac{\mathrm{Tr}\{\exp(-\mathcal{H}_0/kT)\exp[(it/2\hbar)\sum_{j,k}'B_{jk}S_{jx}S_{kx}]S_z\exp[-(it/2\hbar)\sum_{j,k}'B_{jk}S_{jx}S_{kx}]\}}{\mathrm{Tr}\{\exp(-\mathcal{H}_0/kT)\}}$$
$$-\gamma\hbar\sin\omega_0t\frac{\mathrm{Tr}\{\exp(-\mathcal{H}_0/kT)\exp[(it/2\hbar)\sum_{j,k}'B_{jk}S_{jx}S_{kx}]S_y\exp[-(it/2\hbar)\sum_{j,k}'B_{jk}S_{jx}S_{kx}]\}}{\mathrm{Tr}\{\exp(-\mathcal{H}_0/kT)\}}.\quad(40)$$

In the first term of Eq. (40),

$$\exp[(it/2\hbar)\sum_{j,k}'B_{jk}S_{jx}S_{kx}]S_z\exp[-(it/2\hbar)\sum_{j,k}'B_{jk}S_{jx}S_{kx}]=\sum_i e^{iS_{ix}\theta_i}S_{iz}e^{-iS_{ix}\theta_i},\quad(41)$$

where $\theta_i=(t/\hbar)\sum_j' B_{ji}S_{jx}$. (The prime notation indicates the exclusion of the diagonal term $j=i$.) Since $\theta_i$ does not contain any spin operators referring to the $i$th particle, $\theta_i$ commutes with $\mathbf{S}_i$. Therefore, $\exp(i\theta_i S_{ix})$ may be considered to be just a rotation operator for the $i$th particle. Referring to Table I, the first term in Eq. (40) becomes

$$\gamma\hbar\cos\omega_0 t\frac{\sum_i \mathrm{Tr}\{\exp(-\mathcal{H}_0/kT)(S_{iz}\cos\theta_i - S_{iy}\sin\theta_i)\}}{\mathrm{Tr}\{\exp(-\mathcal{H}_0/kT)\}}$$
$$=\gamma\hbar\cos\omega_0 t\sum_i\left(\frac{\mathrm{Tr}\{e^{\zeta S_{iz}}S_{iz}\}}{\mathrm{Tr}\{e^{\zeta S_{iz}}\}}\right)\left(\frac{\mathrm{Tr}\{\exp(\zeta\sum_j' S_{jz})(e^{i\theta_i}+e^{-i\theta_i})\}}{2\,\mathrm{Tr}\{\exp(\zeta\sum_j' S_{jz})\}}\right). \quad (42)$$

From the results of Sec. IIIA, Eq. (42) reduces to

$$\frac{\mu(0)\cos\omega_0 t}{2N_0}\sum_i\left[\prod_j'\left(\frac{\mathrm{Tr}\{e^{\zeta S_{jz}}\exp(itB_{ji}S_{jx}/\hbar)\}}{\mathrm{Tr}\{e^{\zeta S_{jz}}\}}\right)+\prod_j'\left(\frac{\mathrm{Tr}\{e^{\zeta S_{jz}}\exp(-itB_{ji}S_{jx}/\hbar)\}}{\mathrm{Tr}\{e^{\zeta S_{jz}}\}}\right)\right], \quad (43)$$

where, in the product also, the prime notation indicates the exclusion of the diagonal term $j=i$. Expression (43) may be evaluated for any permissible value of $s$ by the following technique. Since the trace is independent of the basis in which it is evaluated, one may use the basis in which the spins are quantized along the $z$ axis. Then

$$\mathrm{Tr}\{e^{\zeta S_{jz}}\exp(itB_{ji}S_{jx}/\hbar)\}$$
$$=\sum_{s'=-s}^{s}\langle\psi_{s'}|e^{\zeta S_{jz}}\exp(itB_{ji}S_{jx}/\hbar)|\psi_{s'}\rangle$$
$$=\sum_{s'=-s}^{s}e^{\zeta s'}\langle\psi_{s'}|\exp(itB_{ji}S_{jx}/\hbar)|\psi_{s'}\rangle. \quad (44)$$

In order to carry out the evaluation of (44), we now express $\psi_{s'}$ as a superposition of wave functions $\phi_{s''}$ for a spin quantized along the $x$ axis, since $\exp[(it/\hbar)B_{ij}S_{jx}]$ working on $\phi_{s''}$ is replaceable by $\exp[(it/\hbar)B_{ij}s'']$ (where $s''=-s$ to $s$). The trace is then expressed in terms of the expansion coefficients of the $\psi_{s'}$ with respect to $\phi_{s''}$.

All further free-induction decay calculations will be performed only for $s=\frac{1}{2}$. For this case it will be more convenient to express the spin operator $\mathbf{S}$ in terms of the Pauli spin operator $\boldsymbol{\sigma}$:

$$\mathbf{S}=\tfrac{1}{2}\boldsymbol{\sigma}.$$

Another method will be used for the evaluation of expression (43) because of its special convenience for the spin $\frac{1}{2}$ case. Using the expansion,[14] $\exp(i\theta\sigma_x)=\cos\theta+i\sigma_x\sin\theta$, expression (43) may be rewritten as

$$\frac{\mu(0)\cos\omega_0 t}{N_0}\sum_{i=1}^{N_0}\prod_j'\cos\left(\frac{B_{ij}t}{2\hbar}\right). \quad (45)$$

Using the same technique, the second term in Eq. (40) may be shown to vanish. Therefore, if $A_{jk}=0$ for all $j$ and $k$,

$$\langle\mu_x(t)\rangle_{\mathrm{Av}}=\mu_0\cos\omega_0 t\frac{1}{N_0}\sum_{i=1}^{N_0}\prod_j'\cos(B_{ij}t/2\hbar). \quad (46)$$

One finds from the above calculation that in the special case in which $A_{jk}=0$ for all $j$ and $k$, $\langle\mu_x(t)\rangle_{\mathrm{Av}}$ may be evaluated without any approximations being made, and that the evaluation predicts a decay shape having beats. This result is not useful for the prediction of actual beat periods, however, because in the case where some $A_{jk}$ are different from zero, the $A_{jk}$ terms wash out those beats predicted by the above expression and introduce others.

### C. General Decay Shapes

From the calculations of the previous section, it appears that the most promising expansion of $\exp[-it(\alpha+\beta)]$ is of the form $\exp(-it\alpha)\chi(t)\exp(-it\beta)$, where $\chi(t)$ is a correction term to take care of the non-commutability of $\alpha$ and $\beta$. The reason for this choice is that the $\exp(-i\alpha t)$ term produces no effect at all upon the free-induction decay, and the effect of the $\exp(-i\beta t)$ term can be evaluated in a closed form.

Since $\alpha$ and $\beta$ are Hermitian operators, and since $\alpha$ commutes with $\sigma_z$ and $\sigma_y$, Eq. (36) reduces to

$$\langle\mu_x(t)\rangle_{\mathrm{Av}}=\frac{\gamma\hbar}{2}\cos\omega_0 t\frac{\mathrm{Tr}\{\exp(-\mathcal{H}_0/kT)e^{i\beta t}\chi^\dagger(t)\sigma_z\chi(t)e^{-i\beta t}\}}{\mathrm{Tr}\{\exp(-\mathcal{H}_0/kT)\}}-\frac{\gamma\hbar}{2}\sin\omega_0 t\frac{\mathrm{Tr}\{\exp(-\mathcal{H}_0/kT)e^{i\beta t}\chi^\dagger(t)\sigma_y\chi(t)e^{-i\beta t}\}}{\mathrm{Tr}\{\exp(-\mathcal{H}_0/kT)\}}. \quad (47)$$

Since $\chi(t)=\exp(i\alpha t)\exp[-it(\alpha+\beta)]\exp(i\beta t)$, $\chi(t)$ may be evaluated by expanding the three exponentials into power series and multiplying the power series together.

$$\chi(t)=c_0+c_1\left(\frac{t}{1!}\right)+c_2\left(\frac{t^2}{2!}\right)+c_3\left(\frac{t^3}{3!}\right)+c_4\left(\frac{t^4}{4!}\right)+\cdots, \quad (48)$$

where the first five coefficients of the power series are

$$c_0=1,\quad c_1=0,\quad c_2=[\alpha,\beta]_-=\lambda,$$
$$c_3=i([\alpha,\lambda]_- - [\beta,\lambda]_-),\quad c_4=c_4'+3\lambda^2,$$

[14] A. Abragam, "Lecture notes on nuclear magnetic resonance," Saclay, 1956 (unpublished).

TABLE II. Traces containing products of $\sigma$ operators.[a] The symbols used include $\eta=2\mu(0)/\gamma\hbar N_0$ and $\phi_{jk}=B_{jk}t/2\hbar$. $\Pi'\cos(\phi_{aj}+\phi_{ak}+\phi_{al})$ means $\Pi_a$ with $a\neq j, k, l$.

| $O_{op}$ | $\mathrm{Tr}\{\exp(-\mathcal{H}_0/kT)e^{i\beta t}O_{op}e^{i\beta t}\}/\mathrm{Tr}\{\exp(-\mathcal{H}_0/kT)\}$ |
|---|---|
| $\sigma_{jz}$ | $\eta\Pi'\cos\phi_{aj}$ |
| $\sigma_{jz}\sigma_{kx}\sigma_{lx}$ | $-\eta\tan\phi_{jk}\tan\phi_{jl}\Pi'\cos\phi_{aj}$ |
| $\sigma_{jz}\sigma_{ky}\sigma_{ly}$ | $-\frac{1}{4}\eta^3[\Pi'\cos(\phi_{aj}+\phi_{ak}+\phi_{al})+\Pi'\cos(-\phi_{aj}+\phi_{ak}+\phi_{al})$<br>$-\Pi'\cos(\phi_{aj}+\phi_{ak}-\phi_{al})-\Pi'\cos(\phi_{aj}-\phi_{ak}+\phi_{al})]$ |
| $\sigma_{jk}\sigma_{ky}$ | $-\eta\tan\phi_{jk}\Pi'\cos\phi_{ak}$ |
| $\sigma_{gx}\sigma_{jy}\sigma_{kx}\sigma_{lx}$ | $\eta\tan\phi_{jg}\tan\phi_{jk}\tan\phi_{jl}\Pi'\cos\phi_{aj}$ |
| $\sigma_{lx}\sigma_{gy}\sigma_{jy}\sigma_{ky}$ | $\frac{1}{4}\eta^3[\sin(\phi_{gl}+\phi_{jl}+\phi_{jl})\Pi'\cos(\phi_{ag}+\phi_{al}+\phi_{ak})$<br>$-\sin(-\phi_{gl}+\phi_{jl}+\phi_{kl})\Pi'\cos(-\phi_{ag}+\phi_{aj}+\phi_{ak})$<br>$-\sin(\phi_{gl}-\phi_{jl}+\phi_{kl})\Pi'\cos(\phi_{ag}-\phi_{aj}+\phi_{ak})$<br>$+\sin(-\phi_{gl}-\phi_{jl}+\phi_{kl})\Pi'\cos(-\phi_{ag}-\phi_{aj}+\phi_{ak})]$ |
| $\sigma_{lx}\sigma_{gy}\sigma_{jz}\sigma_{kz}$ | $-\frac{1}{4}\eta^3[\sin(\phi_{gl}+\phi_{jl}+\phi_{kl})\Pi'\cos(\phi_{ag}+\phi_{aj}+\phi_{ak})$<br>$+\sin(\phi_{gl}+\phi_{jl}-\phi_{kl})\Pi'\cos(\phi_{ag}+\phi_{aj}-\phi_{ak})$<br>$+\sin(\phi_{gl}-\phi_{jl}+\phi_{kl})\Pi'\cos(\phi_{ag}-\phi_{aj}+\phi_{ak})$<br>$+\sin(\phi_{gl}-\phi_{jl}-\phi_{kl})\Pi'\cos(\phi_{ag}-\phi_{aj}-\phi_{ak})]$ |

[a] Traces containing the following operators yielded zero: $\sigma_{jx}$, $\sigma_{jy}$, $\sigma_{jz}\sigma_{ky}\sigma_{lz}$, $\sigma_{jx}\sigma_{ky}\sigma_{lx}$, $\sigma_{jx}\sigma_{kz}$, $\sigma_{lx}\sigma_{gz}\sigma_{jy}\sigma_{ky}$, $\sigma_{lx}\sigma_{kz}\sigma_{gx}\sigma_{jx}$, $\sigma_{lx}\sigma_{kz}\sigma_{gz}\sigma_{jz}$.

and

$$c_4'=[\beta,[\alpha,\lambda]_-]_- - [\alpha,[\alpha,\lambda]_-]_- - [\beta,[\beta,\lambda]_-]_-.$$

The cutting off of the power series at $t^4$ is dictated by the tremendous increase in labor required in order to evaluate any of the terms $c_nt^n$ for $n>4$. Comparison of the theoretical and experimental results will indicate the range of $t$ over which this procedure is valid.

Since $\alpha$ and $\beta$ are Hermitian operators, $c_2^\dagger=([\alpha,\beta]_-)^\dagger=-c_2$. In exactly the same way, one finds that $c_3^\dagger=-c_3$, $(c_4')^\dagger=-c_4$, and $(\lambda^2)^\dagger=\lambda^2$. Therefore, keeping terms up to and including $t^4$,

$$\begin{aligned}\chi^\dagger(t)\sigma_z\chi(t)&\simeq\sigma_z+[\sigma_z,\lambda]_-\frac{t^2}{2!}+[\sigma_z,c_3]_-\frac{t^3}{3!}\\&\quad+([\sigma_z,c_4']_-+3[[\sigma_z,\lambda]_-,\lambda]_-)\frac{t^4}{4!}\\&=P_{z0}+P_{z2}\frac{t^2}{2!}+P_{z3}\frac{t^3}{3!}+P_{z4}\frac{t^4}{4!},\end{aligned}\tag{49}$$

and a similar expression results for $\sigma_y$. Therefore,

$$\begin{aligned}\langle\mu_x(t)\rangle_{\mathrm{Av}}&=\frac{\gamma\hbar}{2}\cos\omega_0t\left(F_0(t)+F_2(t)\frac{t^2}{2!}+F_3(t)\frac{t^3}{3!}\right.\\&\quad\left.+F_4(t)\frac{t^4}{4!}\right)-\frac{\gamma\hbar}{2}\sin\omega_0t\left(G_0(t)+G_2(t)\frac{t^2}{2!}\right.\\&\quad\left.+G_3(t)\frac{t^3}{3!}+G_4(t)\frac{t^4}{4!}\right),\end{aligned}\tag{50}$$

where the $F_n(t)$ coefficients are given by

$$F_n(t)=\frac{\mathrm{Tr}\{\exp(-\mathcal{H}_0/kT)e^{i\beta t}P_{zn}e^{-i\beta t}\}}{\mathrm{Tr}\{\exp(-\mathcal{H}_0/kT)\}}$$

and the $G_n(t)$ by a similar expression.

$F_0(t)$ and $G_0(t)$ are the two terms that describe the induction decay shape for the case $A_{jk}=0$ for all $j$ and $k$. These two terms were evaluated in (IV B). In order to evaluate the higher-order terms, it is first necessary to evaluate some of the commutators in $F_n(t)$ and $G_n(t)$. These commutators have been evaluated in exactly the same way as is $[\alpha,\beta]_-$ in Appendix B, and show that $F_n(t)$ and $G_n(t)$ become more unwieldy and difficult to handle as the subscript $n$ increases. Therefore, only those terms up to and including $F_4(t)$ and $G_4(t)$ were specifically evaluated. The commutators connected with $F_4(t)$ and $G_4(t)$ were not evaluated directly, but rather a procedure was used by which many terms could be discarded on inspection before evaluation.

To find the various $F_n(t)$ and $G_n(t)$ components, one needs to evaluate terms of the form

$$\frac{\mathrm{Tr}\{\exp(-\mathcal{H}_0/kT)e^{i\beta t}O_{op}e^{-i\beta t}\}.}{\mathrm{Tr}\{\exp(-\mathcal{H}_0/kT)\}}\tag{51}$$

$O_{op}$ represents the various products of $\sigma$ operators which occur in $F$ and $G$. The techniques of evaluation fall into two groups. The first is characteristic of that demonstrated in Appendix C for $O_{op}=\sigma_{jz}\sigma_{kx}\sigma_{lx}$. The second technique of evaluation is characteristic of that demonstrated in Appendix D for $O_{op}=\sigma_{jz}\sigma_{ky}\sigma_{ly}$. The results of these trace evaluations are listed in Table II.

Using the evaluated commutators and the traces listed in Table II, one can evaluate $F_2(t)$, $G_2(t)$, $F_3(t)$ and $G_3(t)$. Among the traces are some which have factors $\eta=2\mu(0)/\gamma\hbar N_0$, and some which have factors of $\eta^3$. For $T\geq 0.1$°K and $H_0\leq 10^5$ oersteds, $\eta\ll 1$ for all known nuclei. Those terms which contain a $\eta^3$ factor are therefore dropped. The traces which yield a $\eta^3$ factor contain the product of at least two $\sigma_\alpha$ operators where $\alpha\neq x$. Therefore, on this basis one can drop before evaluation all such terms in $F_4(t)$.

It is seen that for each $\sigma_x$ term to be evaluated in a trace, a tangent term is produced. Since one is only interested in terms independent of $t$ in the $F_4(t)$ and $G_4(t)$ terms (this was previously set as a limit for the order of term desired), one need keep only those terms in the commutator results which contain only a $\sigma_{iz}$. These terms can in general be identified without complete evaluation of the commutator. Evaluating $G_n(t)$, one finds that $G_n(t)=0$ for $n=0$, 2, 3, and 4. It seems reasonable that all the $G_n(t)$ terms should vanish, but thus far this has resisted mathematical proof. Proof of $G_n(t)=0$ for all $n$ is equivalent to showing that an observer in the coordinate system rotating about the $z$ axis with the Larmor frequency $\gamma H_0$ sees the macroscopic magnetization decay without precessing with respect to him.

Evaluation of $F_0(t)$, $F_2(t)$, $F_3(t)$, and $F_4(t)$ yields

$$\langle\mu_x(t)\rangle_{\mathrm{Av}}\simeq\mu(0)\cos\omega_0tQ(t),\tag{52}$$

where

$$\mu(0)=\tfrac{1}{2}N_0\gamma\hbar\tanh(\gamma\hbar H_0/2kT) \quad (53)$$

and

$$Q(t)=\frac{1}{N_0}\Bigg\{\sum_{j=1}^{N_0}\prod_a{}'\cos\left(\frac{B_{aj}t}{2\hbar}\right)+\frac{t^2}{8\hbar^2}\sum_{j\neq k\neq l}A_{jk}(B_{jl}-B_{kl})\times\tan\left(\frac{B_{jk}t}{2\hbar}\right)\tan\left(\frac{B_{jl}t}{2\hbar}\right)\prod_a{}'\cos\left(\frac{B_{aj}t}{2\hbar}\right)$$
$$+\frac{t^3}{48\hbar^3}\sum_{j\neq k\neq l}[2A_{jk}^2(B_{kl}-B_{jl})+2A_{jl}^2(B_{kl}-B_{jk})+A_{jk}A_{kl}(B_{jk}-B_{jl})+A_{jk}A_{jl}(B_{kl}-B_{jk})+A_{jl}A_{kl}(B_{jl}-B_{jk})+A_{jl}A_{jk}(B_{kl}-B_{jl})-A_{kl}(B_{jk}-B_{jl})^2]\tan\left(\frac{B_{kl}t}{2\hbar}\right)\prod_a{}'\cos\left(\frac{B_{al}t}{2\hbar}\right)$$
$$-\frac{t^4}{128\hbar^4}\sum_{j\neq k\neq l}[A_{jk}^2(B_{kl}-B_{jl})^2+A_{jl}^2(B_{kl}-B_{jk})^2+2A_{jk}A_{jl}(B_{kl}-B_{jl})(B_{kl}-B_{jk})]\times\prod_a{}'\cos\left(\frac{B_{ak}t}{2\hbar}\right)\Bigg\}. \quad (54)$$

The function $Q(t)$ is written in a form which is indeterminate for certain values of $t$ (Appendix C). These indeterminacies are introduced through multiplication and division of certain terms by cosine functions. At the points $t_n$ where $Q(t)$ is indeterminate, we may find $Q(t_n)$ by evaluating the limit of $Q(t)$ as $t\rightarrow t_n$.

If one neglects surface effects and considers a lattice in which all the nuclei occupy equivalent lattice positions (such as the fluorine nuclei in $CaF_2$), then $\prod_a{}'\cos(B_{aj}t/2\hbar)$ is independent of $j$, and $Q(t)$ may be rewritten as

$$Q(t)=U(t)V(t), \quad (55)$$

where

$$U(t)=\prod_a{}'\cos(B_{aj}t/2\hbar) \quad (56)$$

and

$$V(t)=1+\frac{t^2}{8\hbar^2}\frac{1}{N_0}\sum_{i\neq k\neq l}A_{jk}(B_{jl}-B_{kl})\tan\left(\frac{B_{jk}t}{2\hbar}\right)\times\tan\left(\frac{B_{jl}t}{2\hbar}\right)+\frac{t^3}{48\hbar^3}\frac{1}{N_0}\sum_{i\neq k\neq l}[-A_{kl}(B_{jk}-B_{jl})^2+4A_{jl}^2(B_{kl}-B_{jk})+2A_{jk}A_{jl}(B_{kl}-B_{jk})+2A_{jk}A_{kl}(B_{jk}-B_{jl})]\tan\left(\frac{B_{kl}t}{2\hbar}\right)$$
$$-\frac{t^4}{64\hbar^4}\frac{1}{N_0}\sum_{i\neq k\neq l}[A_{jk}^2(B_{kl}-B_{jl})^2+A_{jk}A_{jl}(B_{kl}-B_{jl})(B_{kl}-B_{jk})]. \quad (57)$$

Upon examination of the qualifying assumptions made up to this point, one concludes that the free-induction decay formula (52) should hold for all rigid solids containing a single species of spin $\frac{1}{2}$ nuclei. The effects of other nuclear species or of electrons may be taken into account by including their interaction Hamiltonian in $\mathcal{H}_1$ and re-evaluating $\langle\mu_x(t)\rangle_{\text{Av}}$ for the new $\mathcal{H}_1$. The present formulation of the problem has not been limited to spin $\frac{1}{2}$ particles, so one could evaluate formulas for induction decay shapes of particles possessing any spin by following the technique suggested in Sec. IV B.

Van Vleck, in his classic paper,[9] evaluated $\langle\Delta\omega^2\rangle$ and $\langle\Delta\omega^4\rangle$ for a rigid lattice of particles of any spin.

By comparisons of Eq. (26) with Eqs. (52) to (54) for $\langle\mu_x(t)\rangle_{\text{Av}}$, one finds that

$$Q(t)=1-\frac{t^2}{2!}\langle\Delta\omega^2\rangle+\frac{t^4}{4!}\langle\Delta\omega^4\rangle+\cdots. \quad (58)$$

A power series expansion for $Q(t)$ in Eq. (54) reveals that the coefficients of $t^2/2!$ and $t^4/4!$ in (58) coincide respectively with the second and fourth moments predicted by Van Vleck.

### D. Classical Interpretation of the Decay Calculations

Some of the results of the previous quantum-mechanical calculations for free-induction decays can be reproduced from a simple classical model. Although the model does not seem amenable for extension to the general calculation of the decays, it does give some insight into the mechanisms involved.

It will be assumed that the sample under examination contains only one nuclear species with a magnetic dipole moment, that these nuclei have spin $\frac{1}{2}$ and occupy fixed points in space, and that all lattice points are equivalent. As in (IV B), it will be assumed that $A_{jk}=0$ for all $j$ and $k$, so that the total Hamiltonian for the nuclear system may be written as

$$\mathcal{H}=-\gamma\hbar H_0\sum_{j=1}^{N_0}S_{jz}+\tfrac{1}{2}\sum_{j\neq k}B_{jk}S_{jz}S_{kz}. \quad (59)$$

The expectation value of the magnetic field in the $z$ direction at the $j$th nucleus is

$$H_{jz}=\langle\psi|-(\gamma\hbar S_{jz})^{-1}\times(-\gamma\hbar H_0S_{jz}+\textstyle\sum_k{}'B_{jk}S_{jz}S_{kz})|\psi\rangle, \quad (60)$$

where the prime signifies $k\neq j$ and $\psi$ is a suitable wave function for the system of nuclei. We may use the wave functions $\psi$ for which all the spins are individually quantized along the $z$ axis, since such wave functions are eigenfunctions of $\mathcal{H}$. Therefore

$$H_{jz}=H_0-(1/2\gamma\hbar)\sum_k'(\pm B_{jk}). \tag{61}$$

After the "$\pi/2$" pulse there are as many spins up as down along $z$. Thus the probabilities for having a plus or minus sign for $B_{jk}$ in Eq. (61) are each $\frac{1}{2}$.

$\sum_k'(\pm B_{jk})$ can be evaluated by the techniques used for random-walk processes.

The Larmor precession rate of the $j$th nucleus is $\omega_j=\gamma H_{jz}=\omega_0-\Delta\omega_j$, where

$$\Delta\omega_j=\sum_k'(\pm\omega_{jk})=\sum_k'(\pm B_{jk}/2\hbar).$$

From (III B) it can be seen that an induction decay based upon the above model must have the form

$$\langle\mu_x(t)\rangle_{\text{Av}}=\mu(0)\sum_{\Delta\omega_j}P(\Delta\omega_j)\cos(\omega_0-\Delta\omega_j)t, \tag{62}$$

where $P(\Delta\omega_j)$ is the probability that any nucleus (since all the sites are equivalent) will have the Larmor precession rate $\omega_0-\Delta\omega_j$; and where $\mu(0)$ is the value of the macroscopic magnetization immediately after the "$\pi/2$" pulse. $P(\Delta\omega_j)$ is symmetric about $\Delta\omega_j=0$ and, since $\sin\Delta\omega_j t$ is an odd function of $\Delta\omega_j$,

$$\langle\mu_x(t)\rangle_{\text{Av}}=\mu(0)\cos\omega_0 t\sum_{\Delta\omega_j}P(\Delta\omega_j)e^{i\Delta\omega_j t}. \tag{63}$$

However, $P(\Delta\omega_j)=\sum(\frac{1}{2})^{N_0}$, where the sum is to include all states such that $\sum_k'(\pm\omega_{jk})=\Delta\omega_j$. Therefore

$$\begin{aligned}\langle\mu_x(t)\rangle_{\text{Av}}&=\mu(0)\cos\omega_0 t\sum_{\Delta\omega_j}\{(\tfrac{1}{2})^{N_0}\sum(\prod_k' e^{\pm\omega_{jk}t})\}\\&=\mu(0)\cos\omega_0 t\prod_k'(e^{i\omega_{jk}t}+e^{-i\omega_{jk}t})/2\\&=\mu(0)\cos\omega_0 t\prod_k'\cos(B_{jk}t/2\hbar).\end{aligned} \tag{64}$$

Equation (64) is identical to Eq. (52) which was derived quantum mechanically in Sec. IV B for the same set of qualifying conditions used in the present section. The classical interpretation of Eq. (64) is that each nucleus has only a finite number of possible Larmor frequencies, the range of choice of frequencies being the same for each site. The nuclei may be considered to start out in phase at time zero and beat with one another to produce nulls in $\langle\mu_x(t)\rangle_{\text{Av}}$.

Equation (64) illustrates the fact that the assumption by Herzog and Hahn[6] of a Gaussian distribution of local inhomogeneities of $\Delta H_{jz}$ at the lattice sites is not completely justified in the present case. A Gaussian distribution of static local inhomogeneities at the lattice sites would yield a Gaussian-shaped spectral density function and a Gaussian-shaped induction decay, which is in conflict with our experimental results. By using a more complicated summation procedure, which will not be reproduced here, it is possible to show that the correct distribution function for an isochromat of the local field distribution is a Bernoulli function. The distribution function of the local fields over the lattice is a sum of products of Bernoulli functions, which however reduces to a Gaussian function for $B_{jk}\to 0$ and $N_0\to\infty$.

## V. COMPARISON OF THEORY WITH EXPERIMENTAL RESULTS

### A. Predicted Free-Induction Decay Shapes for Calcium Fluoride

Equation (55) can be used to describe the shape of the fluorine induction decay in $CaF_2$ since all the fluorine sites are in this case equivalent. If we make the reasonable assumption that the magnetic interaction between the fluorine nuclei is purely dipolar, then $A_{jk}=-B_{jk}/3$, and Eq. (55) reduces to

$$\langle\mu_x(t)\rangle_{\text{Av}}=\mu(0)\cos\omega_0 t U(t)V(t), \tag{65}$$

where

$$U(t)=\prod_j'\cos(B_{jk}t/2\hbar)$$

and

$$\begin{aligned}V(t)=1&-\frac{1}{6}\left(\frac{t}{2\hbar}\right)^2\frac{1}{N_0}\sum_{i\neq k\neq l}[B_{jk}\tan(B_{jk}t/2\hbar)][B_{jl}\tan(B_{jl}t/2\hbar)]-[B_{jk}\tan(B_{jk}t/2\hbar)]B_{kl}\tan(B_{jl}t/2\hbar)]\\&+\frac{1}{9}\left(\frac{t}{2\hbar}\right)^3\frac{1}{N_0}\sum_{i\neq k\neq l}(2B_{jk}^2B_{kl}-B_{jk}^2B_{jl}-B_{jk}B_{jl}B_{kl})\tan(B_{kl}t/2\hbar)-\frac{1}{12}\left(\frac{t}{2\hbar}\right)^4\frac{1}{N_0}\sum_{i\neq k\neq l}(B_{jk}^2B_{kl}^2-B_{jk}^2B_{kl}B_{jl}).\end{aligned}$$

Terms in $V(t)$ which contain odd functions of $B_{jk}$ are dropped since the sums of these terms over the lattice are negligible compared to the sums of the even functions. Thus,

$$\begin{aligned}V(t)=1&-\frac{1}{6}\left(\frac{t}{2\hbar}\right)^2\frac{1}{N_0}\sum_{i\neq k\neq l}[B_{jk}\tan(B_{jk}t/2\hbar)][B_{jl}\tan(B_{jl}t/2\hbar)]\\&+\frac{2}{9}\left(\frac{t}{2\hbar}\right)^3\frac{1}{N_0}\sum_{i\neq k\neq l}B_{jk}^2B_{kl}\tan(B_{kl}t/2\hbar)-\frac{1}{12}\left(\frac{t}{2\hbar}\right)^4\frac{1}{N_0}\sum_{i\neq k\neq l}B_{jk}^2B_{kl}^2.\end{aligned} \tag{66}$$

Since the fluorine nuclei in a cubic lattice are all equivalent (ignoring surface effects), one can eliminate the indicated summation over $j$ in Eq. (66) and multiply the right-hand side of the equation by $N_0$. By using the relation

$$\sum_{k\neq l} X_k X_l = (\sum_k X_k)^2 - \sum_k X_k^2,$$

Eq. (66) may be rewritten as

$$V(t)=1-\frac{1}{6}\left[\left\{\sum_l{}' \frac{B_{jl}t}{2\hbar}\tan\left(\frac{B_{jl}t}{2\hbar}\right)\right\}^2-\sum_l{}'\left\{\frac{B_{jl}t}{2\hbar}\tan\left(\frac{B_{jl}t}{2\hbar}\right)\right\}^2\right]+\frac{2}{9}\left[\left(\sum_l{}'\left(\frac{B_{jl}t}{2\hbar}\right)^2\right)\left\{\sum_l{}'\frac{B_{jl}t}{2\hbar}\tan\left(\frac{B_{jl}t}{2\hbar}\right)\right\}\right.$$
$$\left.-\sum_l{}'\left(\frac{B_{jl}t}{2\hbar}\right)^3\tan\left(\frac{B_{jl}t}{2\hbar}\right)\right]-\frac{1}{12}\left[\left(\sum_l{}'\left(\frac{B_{jl}t}{2\hbar}\right)^2\right)^2-\sum_l{}'\left(\frac{B_{jl}t}{2\hbar}\right)^4\right]. \quad (67)$$

The above method of writing $V(t)$ has the advantage that all summations are to be taken over a single subscript.

In the evaluation of Eqs. (65) and (67), the terms corresponding to the first 26 near-neighbor fluorine nuclei have been evaluated individually, and the terms corresponding to the more remote nuclei have been coalesced into another sum by a power series expansion. This latter quantity turns out to be isotropic to within $\pm 5\%$ for the orientations considered.

With the use of a fluorine near-neighbor separation of $2.725\times 10^{-8}$ cm in $CaF_2$, free induction decay shapes have been calculated for the cases that $H_0$ is applied along the [100], [110], and [111] axes. The results of these calculations are plotted as the solid curves in Fig. 2 for comparison with the experimental results.

### B. Experimental Free-Induction Decay Shapes for Calcium Fluoride

There are two sets of experimental data to be compared with each other and with the shapes theoretically predicted for the $F^{19}$ decays in calcium fluoride. The first set consists of the actual decay measurements for fluorine in $CaF_2$. The second set is made up of the Fourier transforms of the experimental c.w. line shapes for the same $CaF_2$ crystal.

The rf pulse applied to the sample had a width of five microseconds as measured between half-power points. During the interval of time that the rf pulse is applied, the magnetic dipoles of the sample are being rotated or flipped rapidly by the $H_1$ field, and the magnetic inhomogeneities at the lattice sites are varying at a rate rapid in comparison with the rate at which they can dephase the spins producing the induction signal. Therefore, while the rf pulse is being applied, the macroscopic magnetization is not decaying but has a constant magnitude. The induction decay may therefore be considered to begin at the end of the rf pulse. The experimental free-induction decay measurements are indicated as the crosses in Fig. 2.

As mentioned before, the Fourier-transform data have been derived from experimental c.w. line shapes for $CaF_2$ by use of Eq. (23). The $F^{19}$ c.w. line shapes for our crystal were supplied by Bruce.[8] The Fourier transformation of the c.w. line shape was carried out by the numerical integration of $F(t)=\int g(\omega)\cos\omega t d\omega$ for various values of $t$. $g(\omega)$ is just the normalized function corresponding to the c.w. line shape. The results of these calculations are plotted in Fig. 2 as the open-circle points.

The c.w. line-shape data for calcium fluoride were taken at room temperature; i.e., about 300°K. The induction decay data were taken at both 298°K and 77°K. The 77°K data and the 298°K data were found to agree to within experimental error, so that no distinction has been made between them in the presentations on the graphs or tables.

Table III lists the times, $\tau_n$, at which the decays have nodes; $\tau_n$ refers to the $n$th zero. $N$ stands for no evidence of a zero-point near $\tau_n$.

### C. Discussion

Table III and Fig. 2 show excellent agreement between the experimental induction decay data and the Fourier transforms of the c.w. data at each orientation. These results corroborate the prediction of Eq. (23); *viz.*, if the high-temperature condition is satisfied the shape of the Fourier transform of a c.w. line shape is identical to the corresponding free induction decay.

Figure 2 further shows good qualitative agreement between the experimental decay shapes and the theo-

TABLE III. Locations of nodes on $F^{19}$ free-induction decays in a single crystal of $CaF_2$.[a]

| $H_0$ direction | | $\tau_1$ μsec | $\tau_2$ μsec | $\tau_3$ μsec | $[\langle\Delta\nu^2\rangle]^{-\frac{1}{2}}$ μsec |
|---|---|---|---|---|---|
| [1 0 0] | E | 21.7±1.0 | 42.7±1.7 | 62.7±1.7 | 71.9±4 |
| | F.T. | 22.0 | 43.0 | 63.0 | |
| | Th | 21.8 | 42.5 | 56.7 | 69.7 |
| [1 1 0] | E | 36.9±1.0 | 67.3±1.6 | | 114±4 |
| | F.T. | 37.5 | 68.5 | | |
| | Th | 37.2 | 69.5 | | 112 |
| [1 1 1] | E | 53.8±1.6 | 99.5±3 | | 161±4 |
| | F.T. | 52.0 | 96.5 | | |
| | Th | 60.0 | N | | 164 |

[a] E = direct experimental free-induction decay data. F.T. = Fourier transform of experimental c.w. data. Th = theoretically predicted value. Experimental second moments are those of Bruce.[8] N = no evidence of zero near $\tau_n$.

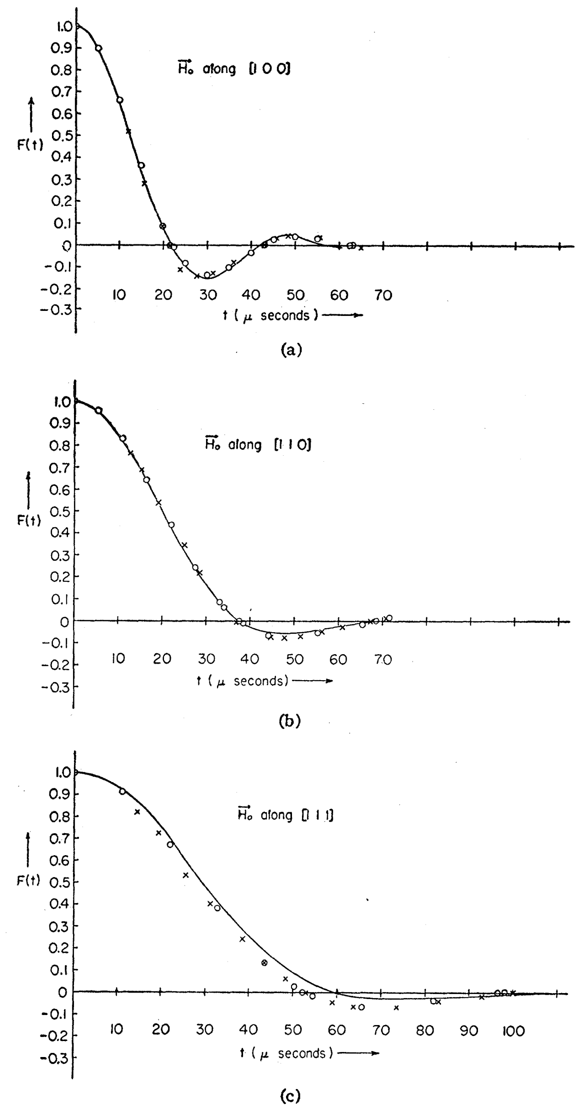


FIG. 2. Bipolar plots of $F^{19}$ free-induction decays in a $CaF_2$ single crystal. (a) $\mathbf{H}_0$ along the [100] axis; (b) $\mathbf{H}_0$ along the [110] axis; (c) $\mathbf{H}_0$ along the [111] axis. The crosses indicate the observed induction decay amplitudes. The circles show the Fourier transform of Bruce's[8] line-shape data for the same crystal. The theoretical induction decays predicted by Eq. (65) are shown as the solid curves.

retically-predicted decay shapes. The best agreement occurs for $\mathbf{H}_0$ along [100] and the poorest for $\mathbf{H}_0$ along [111]. For $\mathbf{H}_0$ along [100] there is excellent agreement between the theoretical and experimental values for $\tau_1$ and $\tau_2$, while the disagreement between the theoretical and experimental values for $\tau_3$ is definitely outside the limits of experimental error. The most probable source of this discrepancy lies in the cutting off of the power-series expansion for $\chi(t)$ at $t^4$ (see IV C). While the theoretically predicted shape of the induction decay may be accurate for small $t$, one expects to obtain poorer results for large $t$ since the higher order terms which have been ignored then make a relatively larger contribution.

Another source of error in the theoretical results arises from the manner in which the induction decay formulas have been evaluated in (V A). There only the first 26 near neighbors were treated individually. The agreement between theory and experiment for reasonably short times corresponds to a successful calculation of all of the $F^{19}$ resonance line shape thus far observable in $CaF_2$. This result has been achieved by explicit consideration of only the first three near-neighbor shells of fluorines and the representation of the contributions from more remote nuclei by a very nearly isotropic function.

Additional sources of discrepancy between the predicted and observed induction decays include misorientation of the crystal and such crystalline lattice defects as vacancies, substitutional impurity ions, and phonons. Because the six nearest $F^{19}$ neighbors to a given fluorine site make no contribution to the local magnetic field at the site for $\mathbf{H}_0$ along [111], it is in just this orientation that the experimental results should be most sensitive to the above sources of deviation from theory. Rough calculations indicate that an 8° rms deviation of the $\mathbf{r}_{jk}$ to the six nearest neighbor $F$ sites is sufficient to bring the theoretical position of the first beat node into agreement with experiment for the [111] direction.

## ACKNOWLEDGMENTS

Several of the electronic circuits used in these experiments were designed and built by Dr. D. E. Maxwell. The authors are indebted to Professor E. Feenberg, Professor G. E. Pake, Professor C. P. Slichter, and Professor J. Townsend for helpful discussions, and to J. Hooper, A. Sher, and L. Smith for their aid in computational work.

The authors are particularly indebted to Professor H. Primakoff for his many stimulating discussions on this problem and to Dr. C. R. Bruce for the use of his line-shape measurements in calcium fluoride prior to their publication.

## APPENDIX A. TIME-DEPENDENT STATISTICAL THEORY

Consider a large number $N$ of identical systems making up an ensemble, each described by the Hamiltonian $\mathcal{H}$. Let the $k$th system be described by the normalized wave function $\psi^k(t)$. This wave function satisfies the Schrödinger equation

$$\mathcal{H}\psi^k(t) = i\hbar\partial\psi^k(t)/\partial t. \tag{A.1}$$

Introduce now a complete set of orthonormal wave functions $\phi_n$ [involving the same coordinates as in $\psi^k(t)$] into which the wave function $\psi^k(t)$ can be expanded.

$$\psi^k(t) = \sum_n a_n^k(t)\phi_n, \tag{A.2}$$

where

$$a_n^k(t)=\int \phi_n^*\psi^k(t)d\tau. \quad (A.3)$$

$\tau$ is a volume element of coordinate space. The coefficient $a_n^k(t)$ can be used to describe the $k$th system.

The density matrix $\rho_{mn}(t)$ is defined as

$$\rho_{mn}(t)=\frac{1}{N}\sum_{k=1}^{N} a_m^k(t)[a_n^k(t)]^*. \quad (A.4)$$

The expectation value of any physical quantity $O$ of the ensemble is found by taking the quantum-mechanical average of $O_{\rm op}$ over the $k$th system and then the average over the ensemble. Thus

$$\langle O(t)\rangle_{\rm Av}=\frac{1}{N}\sum_{k=1}^{N}\int[\psi^k(t)]^*O_{\rm op}\psi^k(t)d\tau. \quad (A.5)$$

Substitute (A.2) into (A.5):

$$\begin{aligned}\langle O(t)\rangle_{\rm Av}&=\sum_{n,m}\left(\frac{1}{N}\sum_{k=1}^{N}(a_n^k(t))^*a_m^k(t)\right)\int\phi_n^*O_{\rm op}\phi_m d\tau\\ &=\sum_{n,m}\rho_{mn}(t)\langle\phi_n|O_{\rm op}|\phi_m\rangle \quad (A.6)\\ &=\mathrm{Tr}\{\rho_{\rm op}(t)O_{\rm op}\}.\end{aligned}$$

It can be shown[15] that for an ensemble in thermal equilibrium, $\rho_{\rm op}(t)$ is time independent and is given by

$$\rho_{\rm op}(t)=\exp(-\mathcal{H}/kT)/\mathrm{Tr}\{\exp(-\mathcal{H}/kT)\}, \quad (A.7)$$

where $T$ is the temperature of the ensemble. Therefore

$$\langle O(t)\rangle_{\rm Av}=\frac{\mathrm{Tr}\{\exp(-\mathcal{H}/kT)O_{\rm op}\}}{\mathrm{Tr}\{\exp(-\mathcal{H}/kT)\}}. \quad (A.8)$$

Assume now that to each system in the ensemble, an identical "shock" (i.e., the $\pi/2$ pulse of Sec. III) is applied. Assume further that this shock is of such form that if the wave function for the $k$th system is $\psi^k(0)$ before the shock, it is

$$[\psi^k(t_w)]'=R_{\rm op}(t_w)\psi^k(0) \quad (A.9)$$

after the shock is turned off, $t_w$ being the length of time the shock lasts. Thus $t$ seconds after the shock is turned off,

$$[\psi^k(t)]''=T_{\rm op}(t)[\psi^k(t_w)]'=T_{\rm op}(t)R_{\rm op}(t_w)\psi^k(0), \quad (A.10)$$

where

$$T_{\rm op}(t)=\exp(-it\mathcal{H}/\hbar).$$

Therefore, $t$ seconds after the shock is turned off:

$$\begin{aligned}\langle O(t)\rangle_{\rm Av}&=\frac{1}{N}\sum_{k=1}^{N}\int\{[\psi^k(t)]''\}^*O_{\rm op}[\psi^k(t)]''d\tau\\ &=\frac{1}{N}\sum_{k=1}^{N}\int[T_{\rm op}(t)R_{\rm op}(t_w)\psi^k(0)]^*\\ &\qquad\times O_{\rm op}[T_{\rm op}(t)R_{\rm op}(t_w)\psi^k(0)]d\tau \quad (A.11)\\ &=\frac{1}{N}\sum_{k=1}^{N}\psi^k(0)[R_{\rm op}^\dagger(t_w)T_{\rm op}^\dagger(t)O_{\rm op}\\ &\qquad\times T_{\rm op}(t)R_{\rm op}(t_w)]\psi^k(0)d\tau.\end{aligned}$$

By substituting (A.2) into (A.11) and proceeding as above,

$$\langle O_{\rm op}\rangle_{\rm Av}=\frac{\mathrm{Tr}\{\exp(-\mathcal{H}/kT)R_{\rm op}^\dagger(t_w)T_{\rm op}^\dagger(t)\times O_{\rm op}T_{\rm op}(t)R_{\rm op}(t_w)\}}{\mathrm{Tr}\{\exp(-\mathcal{H}/kT)\}}. \quad (A.12)$$

## APPENDIX B. EVALUATION OF $[\alpha,\beta]_-$

From Eq. (36)

$$[\alpha,\beta]_-=(1/4\hbar^2)\sum_{i\neq j,k\neq l}A_{ij}B_{kl}[(S_{iy}S_{jy}+S_{iz}S_{jz}),\,S_{kx}S_{lx}]_-. \quad (B.1)$$

To evaluate Eq. (B.1), one must sum over $i$, $j$, $k$, and $l$. Those terms where $i\neq j\neq k\neq l$ vanish since all the operators commute. The only terms left in (B.1) are

$$\begin{aligned}[\alpha,\beta]_-=\frac{1}{4\hbar^2}\sum_{k\neq l}\{&\sum_{j\neq k\neq l}{}_j\,A_{jz}B_{kl}[(S_{ky}S_{jy}+S_{jz}S_{kz}),\,S_{kx}S_{lx}]_-+\sum_{j\neq k\neq l}{}_j\,A_{jl}B_{kl}[(S_{ly}S_{jy}+S_{lz}S_{jz}),\,S_{kx}S_{lx}]_-\\ &+\sum_{i\neq k\neq l}{}_i\,A_{ik}B_{kl}[(S_{ky}S_{iy}+S_{kz}S_{iz}),\,S_{kx}S_{lx}]_-+\sum_{i\neq k\neq l}{}_i\,A_{il}B_{kl}[(S_{ly}S_{iy}+S_{lz}S_{iz}),\,S_{kx}S_{lx}]_-\\ &+2A_{kl}B_{kl}[(S_{ky}S_{ly}+S_{kz}S_{lz}),\,S_{kx}S_{lx}]_-\}. \quad (B.2)\end{aligned}$$

Using the fact that $i$, $j$, $k$, and $l$ are umbric variables and $\mathbf{S}\times\mathbf{S}=i\mathbf{S}$, Eq. (B.2) reduces to

$$[\alpha,\beta]_-=\frac{i}{\hbar^2}\sum_{j\neq k\neq l}A_{jk}(B_{kl}-B_{jl})S_{lx}S_{ky}S_{jz}+\frac{i}{2\hbar^2}\sum_{k\neq l}A_{kl}B_{kl}[S_{ly}(S_{kz}S_{kx}+S_{kx}S_{kz})-S_{lz}(S_{ky}S_{kx}+S_{kx}S_{ky})]. \quad (B.3)$$

[15] D. ter Haar, *Elements of Statistical Mechanics* (Rinehart and Company, New York, 1954), p. 150.

For $S=\frac{1}{2}$, one has $[S_x,S_y]_+=[S_y,S_z]_+=[S_z,S_x]_+=0$ and the second term vanishes in (B.3). Thus for $S=\frac{1}{2}$ and $B_{jk}$ independent of $j$ and $k$, $[\alpha,\beta]_-$ is equal to zero.

## APPENDIX C. EVALUATION OF $\mathrm{Tr}\{\exp(-\mathcal{H}_0/kT)e^{i\beta t}\sigma_{jz}\sigma_{kx}\sigma_{lx}e^{-i\beta t}\}/\mathrm{Tr}\{\exp(-\mathcal{H}_0/kT)\}$

Let $\phi_{jk}=B_{jk}t/4\hbar$. The expression to be evaluated may then be rewritten as

$$\frac{\mathrm{Tr}\{\exp[(\zeta/2)\sum_i\sigma_{iz}]\exp(i\sum_a{}^j\phi_{aj}\sigma_{ax}\sigma_{jx})\sigma_{kx}\sigma_{lx}\sigma_{jz}\exp(-i\sum_a{}^j\phi_{aj}\sigma_{ax}\sigma_{jx})\}}{\mathrm{Tr}\{\exp[(\zeta/2)\sum_i\sigma_{iz}]\}},\tag{C.1}$$

where the notation $\sum_a{}^j$ indicates a summation over $a$ with $a\neq j$. To initiate the evaluation of (C.1), let $a=k$. Since $\exp[i\theta f(\sigma_x,\sigma_y,\sigma_z)]=\cos\theta+if(\sigma_x,\sigma_y,\sigma_z)\sin\theta$ for the case that $f^2=1$, it follows that

$$e^{i\phi_{jk}\sigma_{jx}\sigma_{kx}}\sigma_{jz}\sigma_{kx}\sigma_{lx}e^{-i\phi_{jk}\sigma_{jx}\sigma_{kx}}=\sigma_{lx}(\sigma_{jz}\sigma_{kx}\cos2\phi_{jk}+\sigma_{jy}\sin2\phi_{jk}).\tag{C.2}$$

Therefore (C.1) becomes

$$\sin(2\phi_{jk})\frac{\mathrm{Tr}\{\exp[(\zeta/2)\sum_i{}^k\sigma_{iz}]\exp(i\sum_a{}^{j,k}\phi_{aj}\sigma_{ax}\sigma_{jx})\sigma_{lx}\sigma_{jy}\exp(-i\sum_a{}^{j,k}\phi_{aj}\sigma_{ax}\sigma_{jx})\}}{\mathrm{Tr}\{\exp[(\zeta/2)\sum_i{}^k\sigma_{iz}]\}}.\tag{C.3}$$

If one now lets $a=l$ and repeats the above process, (C.3) reduces to

$$-\sin(2\phi_{jk})\sin(2\phi_{jl})\frac{\mathrm{Tr}\{\exp[(\zeta/2)\sum_i{}^{k,l}\sigma_{iz}]\exp(i\sum_a{}^{j,k,l}\phi_{aj}\sigma_{ax}\sigma_{jx})\sigma_{jz}\exp(-i\sum_a{}^{j,k,l}\phi_{aj}\sigma_{ax}\sigma_{jx})\}}{\mathrm{Tr}\{\exp[(\zeta/2)\sum_i{}^{k,l}\sigma_{iz}]\}}.\tag{C.4}$$

The remaining traces in (C.4) may be evaluated in exactly the same manner that Eq. (40) was evaluated since the two are now identical. Thus expression (C.4) reduces to

$$-\sin(2\phi_{jk})\sin(2\phi_{jl})(2\mu(0)/\gamma\hbar N_0)\prod_{a\neq j,k,l}\cos(2\phi_{aj}).\tag{C.5}$$

If one multiplies and divides expression (C.5) by $\cos(2\phi_{jk})\cos(2\phi_{jl})$, it may be rewritten as

$$-(2\mu(0)/\gamma\hbar N_0)\tan(B_{jk}t/2\hbar)\tan(B_{jl}t/2\hbar)\prod_a{}'\cos(B_{aj}t/2\hbar).\tag{C.6}$$

The trace expressed in the form of Eq. (C.6) is indeterminate at the points where the tangent functions have infinities.

## APPENDIX D. EVALUATION OF $\mathrm{Tr}\{\exp(-\mathcal{H}_0kT)e^{i\beta t}\sigma_{jz}\sigma_{ky}\sigma_{ly}e^{-i\beta t}\}/\mathrm{Tr}\{\exp(-\mathcal{H}_0/kT)\}$

As in Appendix C, let $\phi_{ab}=B_{ab}t/4\hbar$. The expression to be evaluated may then be written as

$$\frac{\mathrm{Tr}\{e^{(\zeta/2)\Sigma_i\sigma_{iz}}e^{(i/2)\Sigma_{a,b}'\phi_{ab}\sigma_{ax}\sigma_{bx}}\sigma_{jz}\sigma_{ky}\sigma_{ly}e^{-(i/2)\Sigma_{a,b}'\phi_{ab}\sigma_{ax}\sigma_{bx}}\}}{\mathrm{Tr}\{e^{(\zeta/2)\Sigma_i\sigma_{iz}}\}}.\tag{D.1}$$

Those terms in (D.1) where $a$ and $b$ are both different from $j$, $k$, and $l$ will vanish since those terms commute with $\sigma_{jz}\sigma_{ky}\sigma_{ly}$. Those terms where $a$ and $b$ are equal to $j$, $k$, or $l$ also vanish, and expression (D.1) may be rewritten as

$$\frac{\mathrm{Tr}\{e^{(\zeta/2)\Sigma_i\sigma_{iz}}(e^{\frac{1}{2}i\sigma_{jx}\theta_j'}\sigma_{jz}e^{-\frac{1}{2}i\sigma_{jx}\theta_j'})(e^{\frac{1}{2}i\sigma_{kx}\theta_k'}\sigma_{ky}e^{-\frac{1}{2}i\sigma_{kx}\theta_k'})(e^{\frac{1}{2}i\sigma_{lx}\theta_l'}\sigma_{ly}e^{-\frac{1}{2}i\sigma_{lx}\theta_l'})\}}{\mathrm{Tr}\{e^{(\zeta/2)\Sigma_i\sigma_{iz}}\}},\tag{D.2}$$

where

$$\theta_l'=2\sum_a{}^{j,k,l}\phi_{al}\sigma_{ax}$$

and $\theta_l'$ commutes with $\boldsymbol{\sigma}_j$, $\boldsymbol{\sigma}_k$, and $\boldsymbol{\sigma}_l$.

From Table I, one finds that (D.2) becomes

$$\frac{\begin{gathered}\mathrm{Tr}\{\exp[(\zeta/2)\sum_i{}^{j,k,l}\sigma_{iz}]\times[\mathrm{Tr}(e^{(\zeta/2)\sigma_{jz}}\sigma_{jz})\cos\theta_j'+\mathrm{Tr}(e^{(\zeta/2)\sigma_{jz}}\sigma_{jy})\sin\theta_j']\times[\mathrm{Tr}(e^{(\zeta/2)\sigma_{kz}}\sigma_{ky})\cos\theta_k'\\-\mathrm{Tr}(e^{(\zeta/2)\sigma_{kz}}\sigma_{kz})\sin\theta_k']\times[\mathrm{Tr}(e^{(\zeta/2)\sigma_{lz}}\sigma_{ly}\}\cos\theta_l'-\mathrm{Tr}\{e^{(\zeta/2)\sigma_{lz}}\sigma_{lz}\}\sin\theta_l']\}\end{gathered}}{\mathrm{Tr}(e^{(\zeta/2)\sigma_{jz}})\,\mathrm{Tr}(e^{(\zeta/2)\sigma_{kz}})\,\mathrm{Tr}(e^{(\zeta/2)\sigma_{lz}})\,\mathrm{Tr}(\exp[(\zeta/2)\sum_i{}^{j,k,l}\sigma_{iz}])}.\tag{D.3}$$

The only terms to survive in (D.3) are of the form

$$\frac{\mathrm{Tr}\{e^{(\zeta/2)\sigma_{jz}}\sigma_{jz}\}}{\mathrm{Tr}\{e^{(\zeta/2)\sigma_{jz}}\}}=\frac{\mu(0)}{\gamma\hbar N_0}.$$

Therefore Eq. (D.3) reduces to

$$\frac{-\left(\dfrac{\mu(0)}{\gamma\hbar N_0}\right)^3 \mathrm{Tr}\{\exp[(\zeta/2)\sum_i{}^{j,k,l}\sigma_{iz}][e^{i(\theta_j'+\theta_k'+\theta_l')}+e^{i(-\theta_j'+\theta_k'+\theta_l')}-e^{i(\theta_j'+\theta_k'-\theta_l')}-e^{i(-\theta_j'+\theta_k'-\theta_l')} -e^{i(\theta_j'-\theta_k'+\theta_l')}-e^{i(-\theta_j'-\theta_k'+\theta_l')}+e^{i(\theta_j'-\theta_k'-\theta_l')}+e^{i(-\theta_j'-\theta_k'-\theta_l')}]\}}{\mathrm{Tr}\{\exp[(\zeta/2)\sum_i{}^{j,k,l}\sigma_{iz}]\}}. \quad \text{(D.4)}$$

The first term of Eq. (D.4) may be evaluated as follows:

$$\theta_j'+\theta_k'+\theta_l'=2\sum_a^{j\,k\,l}\sigma_{ax}(\phi_{aj}+\phi_{ak}+\phi_{al}).$$

Therefore the first term of (D.4) reduces to

$$-\left(\frac{\mu(0)}{\gamma\hbar N_0}\right)^3 \sum_{a\,(a\neq j,k,l)}\left(\frac{\mathrm{Tr}\{e^{(\zeta/2)\sigma_{iz}}[\cos(2(\phi_{aj}+\phi_{ak}+\phi_{al}))+i\sigma_{ax}\sin(2(\phi_{aj}+\phi_{ak}+\phi_{al}))]\}}{\mathrm{Tr}\{e^{(\zeta/2)\sigma_{iz}}\}}\right)$$

$$=-\left(\frac{\mu(0)}{\gamma\hbar N_0}\right)^3 \prod_{a\,(a\neq j,k,l)} \cos[(B_{aj}+B_{ak}+B_{al})t/2\hbar]. \quad \text{(D.5)}$$

If the same procedure is carried out for the other seven terms, Eq. (D.4) reduces to

$$-\frac{1}{4}\left(\frac{2\mu(0)}{\gamma\hbar N_0}\right)^3\Big\{\prod_{a\neq j,k,l}\cos[(B_{aj}+B_{ak}+B_{al})t/2\hbar]+\prod_{a\neq j,k,l}\cos[(-B_{aj}+B_{ak}+B_{al})t/2\hbar]$$
$$-\prod_{a\neq j,k,}\cos[(B_{aj}+B_{ak}-B_{al})t/2\hbar]-\prod_{a\neq j,k,l}\cos[(B_{aj}-B_{ak}+B_{al})t/2\hbar]\Big\}. \quad \text{(D.6)}$$

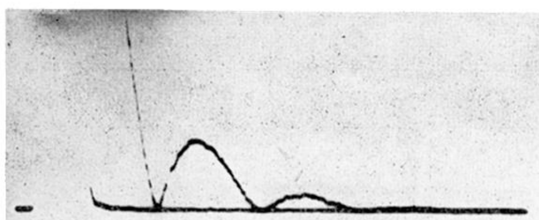

FIG. 1. $F^{19}$ free-induction decay in a $CaF_2$ single crystal. $\mathbf{H}_0$ along [1 0 0]. Temperature 77°K. The visible nulls occur at approximately 22, 43, and 63 $\mu$sec after the rf pulse. The double exposure shows superimposed a second rf pulse which was applied several hundred $\mu$sec after the first pulse in order to check the $\pi/2$ condition of the first pulse. The response to the second pulse also shows a 10-$\mu$sec blocking of the 30-Mc signal amplifier in this case. The beat pattern is distorted by square-law detection.